

The role of *Arabidopsis Thaliana* ribosomal-protein S6 kinase 1
(AtS6K1) under abiotic stresses

Billy Murphy

A thesis submitted for the title of Master of Science (by Dissertation)



School of Life Sciences

University of Essex

Submission date April 25th 2021

Covid-19 Impact statement

The Covid-19 pandemic caused the university labs to close limiting the access and experiments able to take place. The course of research then changed to analysing in house generated data from home. Due to the length of the project, it was decided that the data collected would be sufficient for this thesis considering the limitations. From March 2020 all thesis work was undertaken whilst working from home with all meetings conducted online.

Abstract

Ribosomal protein S6 kinases (S6K) are a family of highly conserved serine/threonine kinases, encompassing two isoforms in plants known as S6K1 and S6K2. Plant S6Ks maintain a similar structure to mammalian and yeast S6Ks, having a high degree of sequence similarity but varying roles. The primary target of S6Ks is the ribosomal protein S6 that forms part of the 40S ribosomal subunit. As such they function as regulators of cell growth, cell proliferation and stress response by regulating protein synthesis and ribosomal biogenesis. Advances in human S6K research has increased exponentially with little focus on plant protein, leaving a large area of fundamental work to be elucidated.

This thesis aims to develop the understanding of plant S6Ks with the structural determination of S6K1. Analysis of in house generated RNA-Seq data showed S6K1 expression to be significantly down-regulated under Heat stress, clarifying previous studies of temporal differences in S6K1 expression. S6K1 transcription factor targets genes were seen to be differentially expressed, upregulating many RBR1 stress-related genes highly enriched in DNA repair. The weak expression of S6K2 transcription factor ABA target genes helps to confirm S6K2s reduced role under heat stress. However, the limited discovery of ABA stress-regulated genes in the literature restricts the clarification of S6K2s function.

Statement of originality

I declare that the work within this document is my own unless stated in the text.

Acknowledgements

Firstly, I would like to thank my supervisor Dr. Ulrike Bechtold for guiding me through my undergraduate research project and onwards through my MSD. She has helped broaden my knowledge of plant biochemistry and enrich my passion in this area. I would also like to thank my supervisor Dr. Filippo Prischi for his support from my undergraduate study to the end of my MSD. He has helped me further my laboratory skills and broaden my knowledge within biochemistry. I would also like to thank the members of both the Prischi and Bechtold lab groups for their moral and scientific support during my time in the lab. I would like to thank my family and friends for their support in my pursuit of a scientific career and their encouragement to keep me motivated throughout my study. And finally, the Christine Desty scholarship for enabling this research to be carried out.

Abbreviations

ABA - Abscisic acid
 AGC – Protein Kinase A,G,C
 AID - Autoinhibitory Domain
 AtLST8 - *Arabidopsis thaliana* Small Lethal with Sec Thirteen 8
 AtPDK1 - *Arabidopsis thaliana* 3-Phosphoinositide-Dependent Kinase 1
 AtRAPTOR - *Arabidopsis thaliana* Regulatory-Associated Protein of TOR
 AtRBR1 - *Arabidopsis thaliana* retinoblastoma-Related 1
 AtS6K1 - *Arabidopsis thaliana* ribosomal-protein S6 kinase 1
 AtS6K2 - *Arabidopsis thaliana* ribosomal-protein S6 kinase 2
 AtTORC1 - *Arabidopsis* TOR Complex 1
 BH - Benjamini-Hochberg value
 bZIPs - Basic zipper transcription factors
 CaMV - Cauliflower mosaic virus
 DDR- DNA damage repair
 DE - Differentially expressed
 DMSO - Dimethyl sulfoxide
 ERK - Extracellular signal-regulated protein kinase
 FDR - False discovery rate
 GST - Glutathione-s-transferase
 HGFM - Hierarchical Graph FM indexes
 HM - Hydrophobic motif
 L2FC- log 2 fold change
 LB - Luria broth
 MRF1 - MA3 Domain-containing translation regulatory factor 1
 mTORC1 - Mammalian Target Of Rapamycin
 NLS - Nuclear Localisation Sequence
 OD - Optical density
 ON - Overnight
 PBS - Phosphate-buffered saline
 PCA - Principal component analysis
 Pchl_a - Protochlorophyllide
 PDK1 - Phosphoinositide-dependent kinase-1
 PIF - PDK1 interacting fragment
 PIKK - phosphatidylinositol 3-kinase-related kinase
 PKA – Protein Kinase A
 PTMs - Post-translational modifications
 RB - Retinoblastoma
 RBR1 - Retinoblastoma related 1
 RISP - Reinitiation-supporting protein
 rpS6 - Ribosomal protein S6
 RT – Room temperature
 S6Ks - p70 ribosomal S6 kinases
 SDS-PAGE - Sodium dodecyl sulphate–polyacrylamide gel electrophoresis
 SnRK1 - Snf1-Related Protein Kinase 1
 TEMED - N,N,N',N'Tetramethylethylenediamine

TF - Transcription factor
TOR - Target of rapamycin
TORC1 - TOR Complex 1
TORC2 - TOR Complex 2
TOS - TOR signalling motif
TPMs - Transcript per million reads
WT - Wild type
WTHS - Wild type heat stress
WTNS - Wild type no stress

Table of Contents

Covid-19 Impact statement.....	2
Abstract.....	3
Statement of originality.....	4
Acknowledgements.....	5
Abbreviations	6
List of tables.....	10
List of figures.....	12
Chapter 1 - Introduction.....	13
1.1 - Introduction.....	13
1.2 - Structure and activation	15
1.3 - TOR.....	20
1.4 - TOR structure and function	21
1.5 - S6Ks roles and targets.....	25
1.5.1 Protein synthesis	25
1.5.2 Hormonal control.....	25
1.5.3 Cell cycle regulatory genes.....	26
1.5.4 Transcription	27
1.6 - AtS6K substrates.....	27
1.7 - Stress and environment.....	29
1.8 - Summary	32
1.9 - Hypothesis, aims and objectives	32
Chapter 2 – Methods and Materials	33
2.1 - Classical cloning.....	33
2.1.1 - PCR Primer design.....	33
2.1.2 – E.coli transformation.....	35
2.1.3 – Plasmid Miniprep and PCR clean-up.....	35
2.1.4 – PCR DNA amplification	36
2.1.5 - Agarose Gel Electrophoresis	39
2.1.6 - Gel Extraction	39
2.1.7 - Double digests of AtS6K1 domains	40
2.1.8 – Ligation of AtS6K1 constructs into pGEX-6p-1 and PET-21a (+) vector.....	42
2.1.9 - Diagnostic digest check	44
2.1.10 - Sequence analysis	46

2.2 – Protein work	46
2.2.1 – Test expression	46
2.2.2 – SDS Page.....	46
2.2.3 – Expression	49
2.2.4 – protein purification.....	51
2.3 – Golden gate cloning	54
2.3.1 – Golden gate primer design	54
2.3.2 – DNA insert PCR amplification	56
2.3.3 – Golden gate protocol	60
2.3.4 - Blue white screening	64
2.3.5 – Colony PCR	64
2.3.6 – Plant growth	69
2.4 – RNA Sequencing.....	69
2.4.1 – RNA-Seq short reads processing.....	69
2.4.2 – Differential expression analysis	70
Chapter 3 - Results	72
3.1 - Cloning of AtS6K1 constructs	72
3.2 - Protein expression of GST tagged AtS6K1 protein	74
3.3 - Protein expression of HIS tagged AtS6K1 protein.....	76
3.4 - Plant gene construction.....	78
3.5.1 - RNA Sequencing output of heat stress <i>Arabidopsis thaliana</i>	80
3.5.2 - Overlapping gene identification experiment	87
3.5.3 - Overlapping gene data retrieval and GO analysis.....	91
Chapter 4 - Discussion	102
4.1 - Protein expression	102
4.2 - Plant work.....	103
4.3 - RNA sequencing	104
4.4 - Conclusion and Future direction	106
References	108
Appendices.....	115

List of tables

Table 2.1. 1.1 Primer properties used for PCR of AtS6K1	34
Table 2.1.4. 1 PCR reaction mixture, volumes and concentrations of reagents	37
Table 2.1.4. 2 PCR program used.....	38
Table 2.1.7. 1 Double digest restriction enzymes, volumes and concentrations of reagents	41
Table 2.1.8. 1 Ligation components volumes and concentrations of reagents	43
Table 2.1.9. 1 Diagnostic digest check volumes and concentrations of reagents	45
Table 2.2.2. 1 SDS-PAGE gel volumes and concentrations of reagents.....	48
Table 2.2.3. 1 Expression media volumes and concentrations of reagents.....	50
Table 2.2.4. 1 HIS tag protein purification buffers volumes and concentrations of reagents	52
Table 2.2.4. 2 GST tag protein purification buffers volumes and concentrations of reagents	53
Table 2.3.1. 1 Primer properties used for PCR of golden gate inserts	55
Table 2.3.2. 1 Primer for insert amplification	57
Table 2.3.2. 2 PCR reaction mixture, volumes and concentrations of reagents	58
Table 2.3.2. 3 PCR program used.....	59

Table 2.3.3. 1 Golden gate reaction mixture, volumes and concentrations of reagents	61
Table 2.3.3. 2 Golden gate constructs insert combination.....	62
Table 2.3.3. 3 Golden gate program used.....	63
Table 2.3.5. 1 Primer properties used for colony PCR of constructs.....	65
Table 2.3.5. 2 Primer combination selected for colony PCR of target constructs.....	66
Table 2.3.5. 3 Colony PCR reaction mixture, volumes and concentrations of reagents	67
Table 2.3.5. 4 Colony PCR program used.....	68
Table 3.5.3. 1 Overlapping TOR related genes with DE heat stress genes	92
Table 3.5.3. 2 Overlapping ABA related genes with DE heat stress genes.....	93
Table 3.5.3. 3 Overlapping top 200 E2F related genes with DE heat stress genes .	94
Table 3.5.3. 4 Overlapping top 200 E2F and RBR1 related genes with DE heat stress genes.....	96
Table 3.5.3. 5 Overlapping RBR1 stress related genes with DE heat stress genes .	97
Table 3.5.3. 6 GO analysis of up-regulated overlapping RBR1 stress related genes with DE heat stress genes.....	101

List of figures

Figure 1. 1 Schematic representation of S6K1 function domains with homology between variants	19
Figure 1. 2 Protein network and pathway of plant AtS6k under stress	24
Figure 3. 1. Cloning of AtS6K1 constructs into vectors	73
Figure 3. 2 Protein expression of GST tagged AtS6K1 protein	75
Figure 3. 3 Protein expression of HIS tagged AtS6K1 protein.....	77
Figure 3. 4 Gene construction for plant vectors.....	79
Figure 3.5. 1 Increased expression of AtS6K1 Gene Chip in <i>Arabidopsis</i>	81
Figure 3.5. 2 Heat map depiction of changes in expression for target groups.....	83
Figure 3.5. 3 Number of up and down-regulated genes	84
Figure 3.5. 4 Volcano plot highlighting significant genes in contrast groups	85
Figure 3.5. 5 Down-regulation of AtS6K1 transcripts	86
Figure 3.5. 6 Overlap of DE genes under HS in WT Col-0 with TOR interacting proteins and plant S6K TF related IDs	89
Figure 3.5. 7 Overlapping plant S6K TF target IDs under compiled stresses and DE genes under Heat stress in WT Col-0.	90

Chapter 1 - Introduction

1.1 - Introduction

The ability to respond to major changes in the external environment is a common characteristic among plants, as extreme conditions such as high temperature, drought, flooding and pathogenic infections can cause major depletions in growth and productivity (Alcázar et al., 2006). These often induce an inability to photosynthesise resulting in energy deprivation and fast but demanding protective mechanisms (Bechtold and Field, 2018a; Beltrán-Peña et al., 2002; Bechtold, Ferguson and Mullineaux, 2018b). As such plants have utilise kinases that function as molecular switches, closely responding to the internal and external environment fine tuning gene expression to the plant's needs (Dobrenel et al., 2016). One identified regulator is the p70 ribosomal S6 kinases (S6Ks), these kinases have been seen in *Arabidopsis thaliana* (*Arabidopsis*) to regulate cell proliferation, cell growth and stress response via modulating ribosomal biogenesis and protein synthesis (Turck, Kozma, Thomas and Nagy, 1998; Mahfouz, Kim, Delauney and Verma, 2005). These are highly significant due to being downstream effectors of the Target Of Rapamycin (TOR), a master regulator of transcription, translation, ribosome biogenesis, translocation of regulatory proteins, autophagy, and storage of reserve compounds (Dobrenel et al., 2016). TOR functions under high nutrient availability in plants, contrasting to Snf1-Related Protein Kinase 1 (SnRK1) that promotes conservation of energy under low carbon conditions (Robaglia, Thomas and Meyer, 2012; Margalha, Confraria and Baena-González, 2019). S6Ks were first identified in 1988 in animals, phosphorylating ribosomal protein S6 (rpS6) (Jeno, Ballou, Novak-Hofer and Thomas, 1988). Only in 1994 were orthologs identified in *Arabidopsis* (Zhang et al., 1994a; Zhang, Lawton, Hunter and Lamb, 1994b). Zhang et al.

(1994b) were able to identify two genes *Ats6k1* and *Ats6k2* (also called *atpk1/atpk6* and *atpk2/atpk19*) from the *Arabidopsis* genome. Generated under a suspected gene duplication from the conserved intron and exon boundaries seen and head to tail tandem array on chromosome 3 (Turck, Kozma, Thomas and Nagy, 1998; Zhang, Lawton, Hunter and Lamb, 1994b).

AtS6K1/2 were suspected to belong to the AGC subfamily however when compared to human PKA, PKC α , and the catalytic kinase domain of S6K1 only produced a 42.29-53.12% sequence identity (Zhang et al., 1994a). The first substrates seen to be phosphorylated was Ribosomal protein S6 (rpS6) when ectopically expressing AtS6K2 in human 293 cells (Turck, Kozma, Thomas and Nagy, 1998). AtS6K1 and AtS6K2 have a degree of sequence similarity of 88.07% which is even greater for the catalytic kinase domain (96.48%). Despite this, their functions are suggested to be different. AtS6K1 is predominantly found in the cytoplasm, while AtS6K2 is localised in the nucleus (Mahfouz, Kim, Delauney and Verma, 2005; Sun et al., 2016). The isoforms mRNA levels also transition with opposite phases: AtS6K1 peaking around dawn and AtS6K2 peaking in the afternoon suggesting alternate functions (Mockler et al., 2007). The specific roles of these isoforms are not yet clear however regulating specific stress response pathways has been suggested (Turck, Kozma, Thomas and Nagy, 1998; Mahfouz, Kim, Delauney and Verma, 2005). Expression of AtS6K1 was induced in response to oxidative, genotoxic and YV-B stresses and downregulated specifically in the roots under osmotic stress. AtS6K2 alternatively has been seen to be overexpressed under high salt levels (Winter et al., 2007). This study aims to gain a comprehensive view of AtS6K1 and in response to stresses, filling in a key area to this research.

1.2 - Structure and activation

The *Arabidopsis* p70 ribosomal protein S6 kinases are serine/threonine kinases in the AGC family. AtS6Ks contain a non-conserved N-terminal regulatory domain, possessing the TOR signalling motif (TOS); a catalytic kinase domain with an activation loop and an AGC C-terminal regulatory region, housing a hydrophobic motif (HM) (Fig. 1.1) (Turck, Kozma, Thomas and Nagy, 1998; Bögre, 2003). The 3D structures of AtS6Ks have not been solved, with no plant AGC kinase domain structures available also. Sequence analysis can be used to determine kinase fold elements. Both AtS6K1 and 2 kinase domains are approximately 256 residues long, containing a predominantly β -sheets N-lobe, with only one α -helix (known as C-helix). A predominantly α -helical C-lobe, with an ATP binding site between the two lobes (Endicott, Noble and Johnson, 2012; Rademacher and Offringa, 2012). An activation segment is present in the C-lobe (DFG-X₁₂-SMCGTTEYMAPE) consisting of the DFG motif, this is required for Mg²⁺ binding, orientating ATP for γ -phosphate transfer, the activation loop (SMCGTTEY) and the APE motif, which mediates the substrate binding (Endicott, Noble and Johnson, 2012; Rademacher and Offringa, 2012). ATP binding is also stabilised by the N-lobe, interacting with a conserved glycine-rich loop (GXGXXG) within. Sequence analyses of AtS6Ks show a single NLS (Nuclear Localisation Sequence) in AtS6K1, situated in the N-terminus of its kinase domain (Mahfouz, Kim, Delauney and Verma, 2005). Contrasting with the two putative NLS located at both ends of the kinase domain in AtS6K2. Expression of AtS6Ks-GFP in BY2 (*Nicotiana tabacum*) cells showed that AtS6K2 is mostly confined within the nucleus, while AtS6K1 is predominantly localised in the cytoplasm, in agreement with the sequence analysis and highlighting the independent functions of the two S6K isoforms in plants (Mahfouz, Kim, Delauney

and Verma, 2005; Henriques et al., 2010). Plant S6Ks activity can be regulated by several factors that influence or directly affect TOR signalling, which includes insulin or insulin-like growth factors (Sánchez de Jiménez, Beltrán-Peña and Ortíz-López, 1999; GARCÍA FLORES et al., 2001), phytohormones such as auxin (Turck et al., 2004; Schepetilnikov et al., 2013; Zhang et al., 2016), nutrients (Zhang et al., 2016) and a range of stress factors (Mahfouz, Kim, Delauney and Verma, 2005), light signals (Turkina, Klang Årstrand and Vener, 2011) and synthetic TOR-S6K specific target compounds (Schepetilnikov et al., 2013).

AtS6K1/2 activation is initiated by the binding of *Arabidopsis* TOR Complex 1 (AtTORC1) to the S6Ks TOS motif, composed of a stretch of 44 amino acid with a 12 amino acid core element different to that of other eukaryotic TOS (Son, Kim, Hur and Cheon, 2017). Three proteins make up AtTORC1 each with individual roles; Firstly AtTOR, a large (~250 KDa) evolutionary conserved serine/threonine protein kinase in the phosphatidylinositol 3-kinase-related kinase (PIKK) family. Secondly the regulatory-Associated Protein of TOR (AtRAPTOR), which influences the substrate specificity and activity of TOR. Finally a small Lethal with Sec Thirteen 8 (AtLST8) protein, incorporated in the TOR-mediated signalling processes (Rexin et al., 2015). TORC1 is the only TOR complex that has been found in plants, contrasting from mammals which contain two TORC1 and TORC2, functionally distinct TOR with high molecular weight complexes (Maegawa, Takii, Ushimaru and Kozaki, 2015).

Direct interaction between AtS6Ks and AtRAPTOR results in AtTOR phosphorylating the T449 and T455 within the HM (**FTNFT_pYVRP**) (bold represents conserved in plants) located on the AGC C-terminal region of AtS6K1 and AtS6K2 (Yaguchi, Ikeya and Kozaki, 2019). This creates a docking site called PDK1 interacting fragment (PIF) (Biondi et al., 2000), identified by *Arabidopsis* 3-Phosphoinositide-Dependent

Kinase 1 (AtPDK1), which binds and phosphorylates AtS6Ks on its activation loop (**S_pMCGTEEY**) (bold represents conserved in plants) on Ser-290 and Ser-296 (Mahfouz, Kim, Delauney and Verma, 2005). This has been shown in AGC kinases to enhance kinase activity by folding back on to the N-lobe kinase domain (Rademacher and Offringa, 2012), but nothing has been published on plants. The activation loops phosphorylation is well characterised with a conserved priming mechanism that enables these kinases to phosphorylate their substrates (Kannan, Haste, Taylor and Neuwald, 2007). Prior to phosphorylation, the activation loop is usually disordered, preventing substrate binding (Nolen, Taylor and Ghosh, 2004). Once phosphorylated the activation loop promotes H-bonds binding with the C-helix and the activation segment, this induces an “open” structure conformation which allows the binding and phosphorylation of Mg²⁺ and substrates respectively (Huse and Kuriyan, 2002). Other post-translational modifications (PTMs) have been seen in human S6Ks, but studies on plants are limited, so there is no available information about the presence and roles of additional PTMs on AtS6Ks.

Despite a large sequence similarity and functional conservation with the human S6Ks (Turck, Kozma, Thomas and Nagy, 1998), the activation mechanism is significantly different for plants. Human S6Ks are activated by ERK (extracellular signal-regulated protein kinase), which targets the C-terminal autoinhibitory domain resulting in phosphorylation, which is not present in plants S6Ks (Pardo and Seckl, 2013). This induces a conformational change allowing TORC1 and PDK1 (Phosphoinositide-dependent kinase-1) to phosphorylate their targets (Pardo and Seckl, 2013). This could indicate that the kinase domain has an evolutionarily conserved function (Turck, Kozma, Thomas and Nagy, 1998) and a species-specific substrate selection via the N- and C-terminal of the protein (Rademacher and

Offringa, 2012). Regulatory differences between plant and human S6Ks have been seen in *Arabidopsis*, rice, soybean, maize and tomato (Yaguchi, Ikeya and Kozaki, 2019).

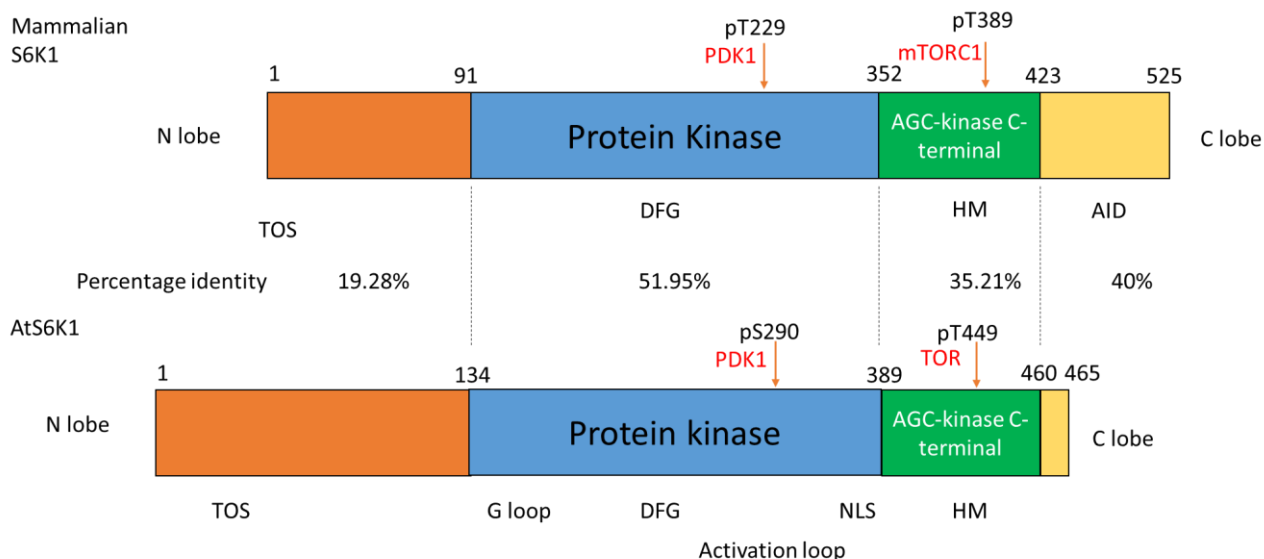


Figure 1. 1 Schematic representation of S6K1 function domains with homology between variants

Primary structure comparison of mammalian and plant S6K1 variants with a schematic of amino acids percentage amino acid identity. The N-terminal Domain is orange; protein kinase is blue; C-terminal AGC kinase depicted in green and the non-conserved C-terminal domain is yellow.

TOS, Target of rapamycin signalling motif; HM, Hydrophobic Motif; AID, Autoinhibitory Domain; G loop, Glycine rich loop; NLS, Nuclear Localisation Sequence; PDK1, 3-phosphoinositide dependent protein kinase-1; mTORC1, mammalian Target Of Rapamycin and TOR, Target Of Rapamycin.

1.3 - TOR

TOR is the master regulator of protein production in eukaryotes, it controls ribosome biogenesis, translation and transcription (Rexin et al., 2015). TOR was first identified in yeast over 20 years ago as a growth enabling protein kinase, which was then later discovered in all major eukaryote groups (Vézina, Kudelski and Sehgal, 1975). The discovery of TOR was elucidated by the presence rapamycin a compound produced by a soil bacterium *Streptomyces hygroscopicus*, first found to be an antifungal and then later as a potential immunosuppressant and growth inhibitor (Vézina, Kudelski and Sehgal, 1975). It has interactions with a large protein in yeast was later identified as TOR. Alike S6Ks TOR is a serine/threonine kinase but belonging to the PIKKs family (Engelman, Luo and Cantley, 2006).

TOR functions as a regulatory pathway responding to a whole host of stimuli such as energy, stress and nutrients in order to carry out the desired response in growth and metabolism. TOR activity is highly conserved across different organisms with individual growth strategies adapting for each case. Since the discovery of TOR its complexity has continued to expand from the simple control of a single celled yeast on growth and cell division, to greater complexity multicellular organisms. Thus usually maintaining similar features with additional units commonly involved with metabolism-related disease and cancer (Rexin et al., 2015).

TOR in plants is thought to be more complex with the need to diverge from mammalian like heterotrophic energy utilisation for seed development, transitioning to chloroplast driven autotrophic metabolism and inorganic nutrient uptake from roots (Rexin et al., 2015). The ability for plants to respond to environmental cues and change their physiology is an underpinning ability to ensure survival for an immobile kingdom.

1.4 - TOR structure and function

TOR has protein to protein and protein to membrane interactions that are associated with its highly conserved HEAT repeats. The kinase activity of TOR is attributed to the combination of the FAT domain, kinase domain and the C-terminal FAT domain (Rexin et al., 2015). The final FRB domain is involved in the inhibition of action when targeted by the FKBP12-rapamycin complex. This causes growth arrest, reduced protein synthesis and simulating starvation in mammals. These structures, however, are not necessarily needed when observed in plants, with the FATC domain having no phenotypic change with its removal. The Expression of the kinase domain alone could rescue the function of TOR with a compromised kinase domain, suggesting an independent or autonomous function (Rexin et al., 2015).

In animals and yeast, TOR is found in two large protein complexes that recruit different substrates. One of which is sensitive to rapamycin known as TOR complex 1 (TORC1) that contains TOR (TOR1 or TOR2 in yeast), mLST8/G β L proteins and RAPTOR/KOG1; the second phosphorylates Akt/PKB in animals and is known as TOR complex 2 (TORC2), consisting of TOR (TOR2 in yeast), mLST8/G β L and Rictor/AVO3 (Deprost et al., 2007).

The existence of several components of the TOR signalling path has been identified in plants with complexes such as RAPTOR (a TOR regulatory protein) and mLST8/G β L proteins also being present. Very little is known about these proteins with the function of LST8 still unknown. However, it is necessary for RAPTOR dependent activation of TOR (Deprost et al., 2007). TORC1 has a well-established link with equivalents of RAPTOR in plants, this could be due to its role in polarised growth, therefore allowing plants to grow by characterised hydrostatic driven expansion and cytoskeleton development (Sarbasov, 2005). The deficiency of LST8

protein in *Arabidopsis* during long days results in slowed growth and greater branching possibly responding to photosynthetic variation (Rexin et al., 2015).

Plant resistance to rapamycin made initial research difficult by relying on genome-based work, this was overcome in recent years with the knowledge that rapamycin binds FKBP12 and enable inhibition of TOR. Under increased activity of TOR results in increased cellular size and greater root and shoot growth, with correlating negative association under reduced activity. Other effects of down-regulation include altered branching, cell wall synthesis, reduced meristem cell division and root hair development (Ren et al., 2012; Feldman et al., 2009).

The allocation of metabolites is the key factor in TOR regulated growth or energy storage as seen by tricarboxylic acid cycle intermediates, triglyceride and starch accumulation in TOR inhibited or LST8 mutated *Arabidopsis*. Similarly, as with nitrogen metabolism under inactivation of a PP2A binding protein TAP42.

Inactivation of TOR also leads to amino acid accumulation suggesting autophagy and reduced protein synthesis and the reduced oxygen radical scavengers (Ahn et al., 2011). TOR has also been seen to have roles in the regulation of translation with its kinase domain interacting with rRNA promoter regions. Its involvement further stems from its influence on translation reinitiation from TOR activated S6K, which phosphorylates eIF3H (eukaryotic initiation factor 3H) that helps the ribosome to mRNA interaction past stop codons to downstream ORFs (Rosado et al., 2012).

TOR can regulate several cellular components directly or via the phosphorylation of two main downstream effectors, eIF 4E-binding protein and S6Ks (Shin et al., 2012). It has been shown that RAPTOR1 can interact with the HEAT repeats of TOR and is known to also regulate S6K activity under osmotic stress. Interestingly the putative substrate AtS6K1 to TOR has also been observed to interact with RAPTOR1. S6K1

has been shown to effectively phosphorylate *Arabidopsis* ribosomal S6 protein with S6K1 catalytic ability being dependent on its phosphorylation by *Arabidopsis* PDK1. Under osmotic stress, S6K1 activity is affected however it has no impact on PDK1 activity (Mahfouz et al., 2005). Furthermore, increased production of RAPTOR1 results in the relief of this stress. This supports the potential presence of an equivalent TOR kinase pathway present in plants (Fig 1.2) (Shin et al., 2012).

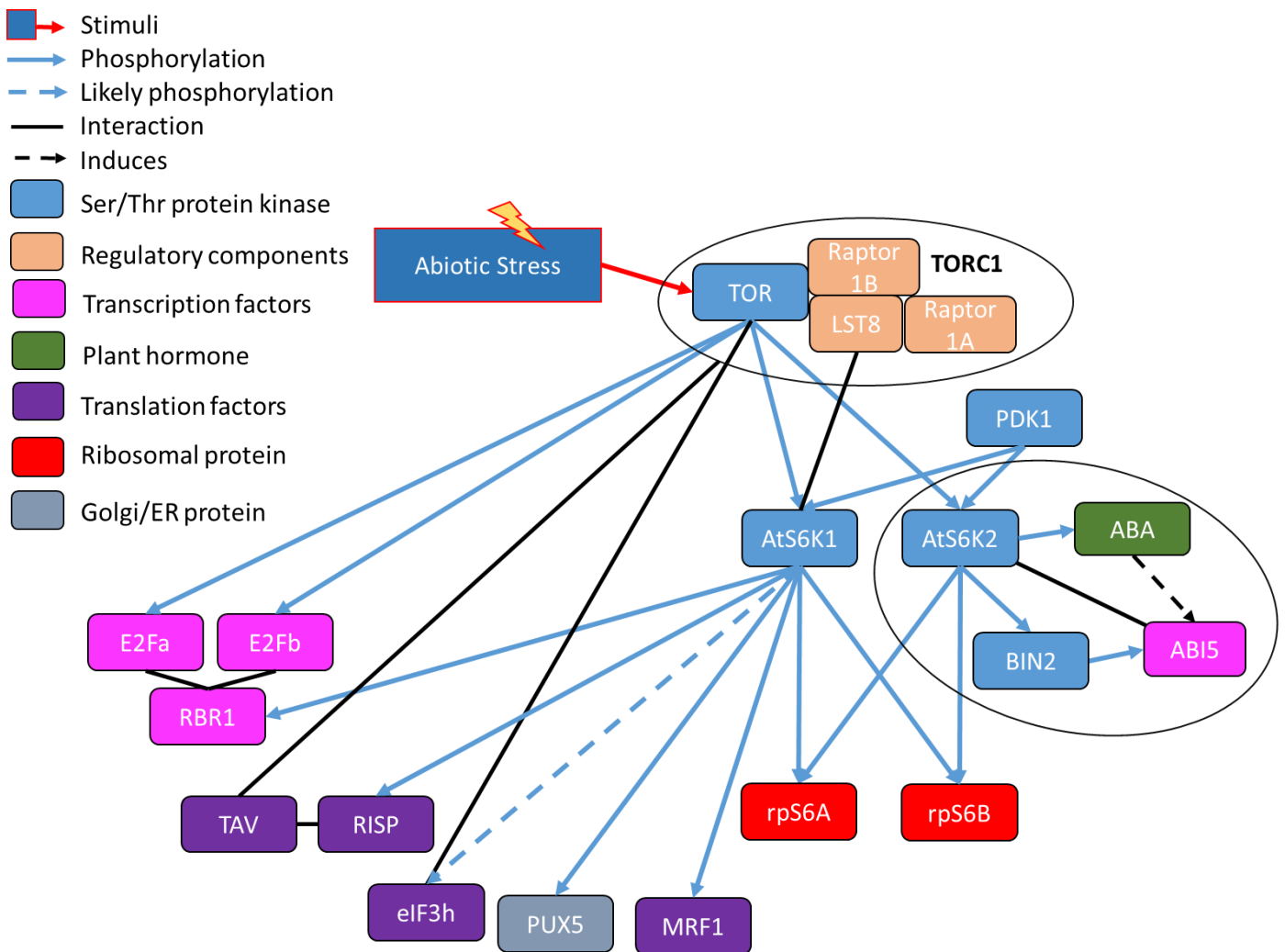


Figure 1. 2 Protein network and pathway of plant AtS6k under stress

The red arrow and dark blue box depict environmental stimuli, blue arrows depict phosphorylation, black dotted arrows depict induction, dotted blue arrows as proposed phosphorylation and black lines as interactions. Blue boxes resemble Ser/Thr kinases, orange boxes are regulatory components, pink depicts transcription factors and purple as translation factors. The grey box depicts Golgi/ER protein and the red box resembles Ribosomal protein.

1.5 - S6Ks roles and targets

The phosphorylation target motif of S6Ks has been identified as RXRXXS/T, this sequence is conserved throughout the AGC kinase family and gives insight into protein interactions from known libraries (Tavares et al., 2015). The primary target of S6Ks is the ribosomal protein S6 that forms part of the 40S ribosomal subunit (Mahfouz et al., 2005). This makes S6Ks role imperative to protein synthesis with it influencing the key biological machinery involved (Piques et al., 2009). This enables ribosomal function with the recruitment of transcripts and the generation of a polysome to occur. Regarding plants, very little research has been completed in this area with only a handful of genes being understood concerning rate of growth and plant body size (Deprost et al., 2007)

1.5.1 Protein synthesis

The deficiency of S6Ks have some similar roles among different organisms, one such example dS6K in *Drosophila* that leads to reduced cell size and an extreme delay in development leading to embryonic lethality (Montagne, 1999). This was similarly observed in yeast during increased levels of ribosome biogenesis and protein synthesis, showing the phosphorylation of its S6K1 homolog influences life span and cell size. *Arabidopsis* AtTOR knockout mutants also gave the same phenotype (Sengupta, Peterson and Sabatini, 2010).

1.5.2 Hormonal control

One rather exciting development is the discovery of certain phytohormones ability to influence the TOR signalling pathway, both Auxin and cytokinin being able to activate AtS6K1 in suspension cells (Turck et al., 2004). The induction of AtS6K1 by

auxin resulted in the suppression of cell cycle regulatory genes and also increased calli size of transgenic plants, resulting in a 30% larger cell mass (Shin et al., 2012). However, in protoplasts this relationship appears to be reversed, increasing the expression of cell cycle regulatory genes. This hints at potential other regulatory circuits in relation to the cells physiological or spatial status (Turck et al., 2004). Sensitivity to abscisic acid (ABA) has also been seen to correlate with overexpressed or silenced lines of AtTOR (Turck et al., 2004; Deprost et al., 2007).

1.5.3 Cell cycle regulatory genes

The ability of AtS6K1 to positively regulate cell size has recently been observed from inhibiting the expression of mitotic CYCB1;1 this gave a reduction of cell size and ploidy from RNAi-based AtS6K suppression (Henriques et al., 2010). This has also been recently supported by Shin et al. (2012). Finding that along with mitotic CYCB1;1 many other cell cycle regulatory genes are also down-regulated under increase expression of AtS6K1. These include the G1-specific CYCD3;1, the S phase-specific RNR2, the G2/mitotic-specific CYCB1;1, and the plant-specific CDKB1;1 gene. The only morphological phenotype observed is the presence of a longer root tip in seedlings, likely due to the increase in accumulation of AtS6K1 from greater localised tip auxin concentration.

Interestingly AtS6K1 has also been seen to associate with a plant variant of retinoblastoma (RB) protein known as RBR1, which acts in repressing cell proliferation (Henriques et al., 2010). Under the phosphorylation of this protein results in its nuclear localisation, where it functions by inhibiting E2F transcription factor activity (Henriques et al., 2010). This phosphorylation results in the silencing of needed cell cycle-related genes. Recent studies have also suggested that TOR

could further regulate cell division via E2Fa phosphorylation, potential being a direct target for TOR (Rexin et al., 2015).

1.5.4 Transcription

Interestingly there have been correlations seen between the transcription of AtS6K1 and endogenous AtS6K2. Under increased transcription of the transgenic AtS6K1 also increased transcription of AtS6K2. This suggests a potential cross-talk mechanism between the two S6K genes (Shin et al., 2012).

1.6 - AtS6K substrates

The phosphorylation target sequence of S6Ks is conserved within the AGC kinase family, enabling phosphorylation on recognition of as mentioned RXXXS/T sequence (Tavares et al., 2015). The primary target and most well clarified is the rpS6. Two functionally equivalent forms of rsS6 have been identified in *Arabidopsis*, rpS6A and rpS6B (Chang, Szick-Miranda, Pan and Bailey-Serres, 2005; Creff, Sormani and Desnos, 2010). rpS6 occupies the mRNA/tRNA binding site of the 40s subunit, being the only protein in the subunit that is controlled via phosphorylation (Mahfouz et al., 2005). Cap-dependent translation is increased under rps6 phosphorylation however this is not fully understood (Enganti et al., 2018). Research in maize has suggested that rpS6 phosphorylation regulates the translation of specific proteins downstream of auxin stimulation 5'TOP-like mRNAs being located into polysomes under auxin stimulation (Beltran-Pena et al., 2002; Levy et al., 1991). rpS6 is most commonly phosphorylated on residues S237 and S40 in plants (Enganti et al., 2018; Williams et al., 2003) with varying levels under day and night transitions (Turkina, Klang Årstrand and Vener, 2011). Turkina, Klang Årstrand and Vener,

(2011) also discovered a novel phosphorylation site S231 under broad mass spectrometry analysis of *Arabidopsis* cytosolic rps6. Day to night variation saw phosphorylation on S231, S237 and S240 being 2.2, 4.2 and 1.8 times increase respectively, likely in response to the greater metabolic demand of the light period (Turkina, Klang Årstrand and Vener, 2011). In humans, S6Ks phosphorylate rpS6 on S235 (*Arabidopsis* S240 equivalent), S236, S249 and S244. In addition, RSKs also phosphorylate S235 and S236 that are not present in plants (Roux et al., 2007). In *Arabidopsis*, S6Ks are key players of reinitiation and translation with the phosphorylation of MRF1 (MA3 DOMAIN-CONTAINING TRANSLATION REGULATORY FACTOR 1) under increased cellular energy downstream of AtTOR-AtS6Ks (Lee, Park, Ahn and Pai, 2017).

The MRF family genes (MRF1-MRF4) are regulated by TOR, influencing translation activity (Lee, Park, Ahn and Pai, 2017). The association of MRF1 with eIF4A-1 is observed under glucose and light conditions, this enables ribosome scanning via catalysing the unwinding of mRNA by eIF4A-1 at the 5'-UTR under favourable conditions (Lee, Park, Ahn and Pai, 2017).

Phytohormone auxin treatment has been shown to cause AtTORC1 to associate with polysomes phosphorylating inactive bound AtS6K1, inducing the phosphorylation of eIF3h (Schepetilnikov et al., 2013). This in turn increases their action of ribosomal loading of uORF-containing mRNAs, promoting the translation of basic zipper transcription factors (bZIPs) and auxin response factors (ARFs) (Schepetilnikov et al., 2013; Kim et al., 2004).

Similarly, the reinitiation factor of Cauliflower mosaic virus (CaMV) TAV has been shown to bind and activate AtTOR. This induces polysome association and the phosphorylation of AtS6K1 further phosphorylating the reinitiation-supporting protein

(RISP), in which TAV binds on the association to the polysome. This enables needed biological machinery to be present for translation of downstream ORFs after termination (Schepetilnikov et al., 2011; Thiébeauld et al., 2009). Nutrient limiting conditions have shown AtS6K1 to repress proliferation by activating and binding to *Arabidopsis thaliana* retinoblastoma-Related 1 (AtRBR 1), a known inhibitor of E2F transcription factors (Henriques et al., 2010; van den Heuvel and Dyson, 2008). Whether other AtS6Ks could act similarly is unclear however with the presence of a LxCxE motif being seen on AtS6K2 could indicate it does so (Henriques et al., 2010).

1.7 - Stress and environment

The ability to regulate and buffer cellular stress generally results in damaging effects, including ageing, diabetes and tumorigenesis. Cells use this as a way to dissipate the incoming threat but maintaining function. The coordination of physiological, biochemical and behavioural aspects of living organisms is paramount to survival with big fluctuations in activity and process from diurnal cycles (Piques et al., 2009). Plants heavily rely on the development of their circadian clocks to regulate the majority of their biological processes, compared to the rapid responses as seen in mammals. Responses to sugars and day and night changes also play a key role in the up or downregulation in phosphorylation, controlling many key transcripts (Piques et al., 2009). This is true for rates of protein synthesis seen in *Arabidopsis* with an increase of 50-150% during the daylight photoperiod compared to the dark period, correlating with the activity increase of 50-100% for light-stimulated associated enzymes. This also correlates with the reduced ribosomal concentration seen during plant dark periods, however very little is known regarding the molecular

mechanisms for these diurnal variations (Piques et al., 2009). With this response, the production of transcripts in plants is relatively fast compared to protein production, with transcript production being synthesised within hours. The period until significant levels of protein have been produced is still several days later (Piques et al., 2009).

To enable a rapid response for protein translation in eukaryotes a typical series of protein phosphorylation events is present. This differs in higher plants with the rapid fluctuations being heavily supported by the changes in the phosphorylation status of ribosomal protein S6, this has been seen in response to variations in environmental conditions (Turck et al., 2004).

Cold stress has been seen to be one of these factors with the accumulation of a hyper-phosphorylated version of the S6 protein being found in the root tips of maize, however being reduced in response to heat shock and oxygen deprivation (Williams et al., 2003). This correlates with the increase in AtS6K1 and AtS6K2 transcripts that become further upregulated in the presence of cold stress in *Arabidopsis* seedlings. Interestingly Mizoguchi et al. (1995) also showed cold stress increased mRNA levels but was also increased by salt and drought stress.

The presence of heat stress also showed a positive correlation to the phosphorylation of S6 and polysome accumulation of ribosomal protein transcripts (Beltran-Pena et al., 2002). In cell suspension cultures of tomato exposed to heat shock resulted in the rapid but reversible decline of the phosphorylation status of ribosomal protein S6 above temperatures of 35 degrees C. This coincides with the decrease in cellular proliferation via a lower mitotic index and the synthesis of heat shock proteins (Scharf and Nover, 1982).

Khandal et al. (2009) found that in barley during illumination periods protochlorophyllide (Pchl_{id}) was accumulating and functioning as a photosensitive switch triggering the production of singlet oxygen and cell death. Both Pchl_{id} and singlet oxygen production has been linked to the control of metabolite accumulation and gene expression, with the suppression of ribulose-1,5-bisphosphate carboxylase/oxygenase small and large subunits production, photosystem II chlorophyll a and b binding protein and other associated proteins. This is primarily caused by the halt in translation initiation of 80S cytoplasmic ribosomal photosynthetic transcripts, however, that also correlated with the decline in the phosphorylation status of ribosomal S6 protein.

Variations in environmental stress conditions have been seen to influence and noticeably reduce the growth of *Arabidopsis* suspension cells. Under treatment with sugar starvation or osmotic stress resulted in growth retardation, however from substrate-mediated kinase pull down had no effect on the kinase activities for AtS6K1 phosphorylation. Interestingly during a combined stress test when both starvation and osmotic stress were acting together resulted in a decrease in the phosphorylation of these domains. This does not align with current knowledge of S6K1 however this could be due to the high auxin concentration present in the media, which has been seen to stimulate AtS6K activity. What is most interesting however is the fact that both osmotic and starvation stresses were needed in conjunction to elicit a response. This suggests that these signals could function separately but are both needed to influence the phosphorylation of AtS6K1 (Shin et al., 2012).

1.8 - Summary

In conclusion, S6Ks are multi-role ribosomal kinases present in both mammalian and plant systems. Having roles in many factors such as growth, metabolism and stress response. However, the extent to which the plant variant AtS6K plays is not well understood. I aim to clarify the interactions of AtS6K1 with potential partners, further elucidate its role in stress signalling from heat stress RNA sequencing data.

1.9 - Hypothesis, aims and objectives

We hypothesised that in order to respond effectively to stress conditions AtS6K1 and AtS6K2 target different transcription factors to regulate needed cellular protein machinery. As such, the aim of this project is to identify and determine the genomics relating to AtS6K1 under stress conditions, focusing on the S6K1 isoform-specific roles.

Aim: Determine gene expression of AtS6K isoforms under heat stress.

In house generated RNA sequencing data will be analysed with overlapping genes of interest. Identifying significantly differentially expressed genes under heat stress conditions.

Chapter 2 – Methods and Materials

2.1 - Classical cloning

2.1.1 - PCR Primer design

The AtS6K1 gene sequences were obtained from the protein database NCBI. These sequences were then used to design primers for specific contrast DNA amplification via PCR and ligation with pGEX-6p-1(N-terminal GST) and Pet-21a (+) (C-terminal His) vectors. The primers were designed to 20 -30 bp reducing aspecific binding events. GC and Tm values that were calculated ensuring increased G-C bases for GC clamp and Tm to increase annealing efficiency. Limited similarity between the primers was ensured to prevent primer dimer formation.

The forward and reverse primer pairs all had melting temperatures similar to each other. Closer melting temperatures increase specific binding to the template and increases PCR efficiency, due to primers annealing around the same temperature. Table 2.1.1.1 shows the forward (Fwd) and reverse (Rvr) designed primer sequences, their recognised restriction enzyme, the annealing temperatures for PCR and chemical properties (ThermoFisher Tm calculator).

Table 2.1. 1.1 Primer properties used for PCR of AtS6K1

GC% and T_m value were calculated using an online tool (T_m Calculator). Forward primers are indicated by (F) and reverse primers are indicated by (R).

Primer	length	T _m (°C)	GC %	Sequence (5'-3')
AtS6K1_1_ EcoRI (F)	25	70.6	48	CGTGAATCATGGTGTTCATCTCAGC
AtS6K1_113_ EcoRI (F)	27	72.6	44.4	CGTGAATTCGATAACGAAAAGGCCTTG
AtS6K1_408_ XhoI (R)	27	73.3	51.8	CGTCTCGAGTTATGGTTTGAAGCTCGG
AtS6K1_465_ XhoI (R)	29	71.0	48.2	CGTCTCGAGTTACAAGGTCGTAGTGGATT
AtS6K1_408_nost op XhoI (R)	24	73.6	58.3	CGTCTCGAGTGGTTTGAAGCTCGG
AtS6K1_465_nost op XhoI (R)	26	72.6	53.8	CGTCTCGAGCAAGGTCGTCTGGATT

2.1.2 – *E.coli* transformation

1 µl of plasmid DNA or 5 µl of ligation mixture was added to 50 µl of BL21 (DE3) *E. coli* cells or DH5α *E. coli* cells (Thermo scientific) for DNA amplification and further incubated on ice for 30 minutes. Cells were then subjected to a heat shock at 42°C for 45 seconds using a water bath and further kept on ice for 2 minutes. 500 µl of Luria Broth (LB) (or 200 µl for ligation) was then added to the cells, before being incubated at 37 °C for an hour with shaking. Cells were then diluted in 10 ml of LB for amplification, spread on LB agar plates for ligation; 100µg/ml Ampicillin for both LB and LB agar plates with an additional 100µg/ml of X-Gal for blue-white screening. Cultures and plates were incubated overnight (ON) at 37°C with shaking for culture only. Air contamination was limited using a class II microbiological safety cabinet where possible during air exposure to cells.

2.1.3 – Plasmid Miniprep and PCR clean-up

Thermo Scientific GeneJet Plasmid miniprep kit was used to carry out miniprep. Thermo Scientific Heraeus Megafuge 40R bench top centrifuge was used to centrifuge cell cultures for 10 minutes at 4000G. The supernatant was then discarded, and the pellet re-suspended in 250 µl of resuspension buffer. Samples were then lysed with 250 µl of Lysis buffer followed by 350 µl of neutralisation buffer added, inverting after each addition. Thermo Scientific minispin microcentrifuge was used centrifuging at 11,400G for 10 minutes. The supernatant was then extracted from the sample and transferred to a miniprep column and centrifuged for one minute at 11,400g. The plasmid sample or prepared PCR samples with 5x sample volume of binding buffer added for PCR clean-up, was washed twice with 500 µl of wash buffer and centrifuged for one minute at 11,400g per wash. A two minute spin

at 11,400g was then carried out removing residual wash ethanol and then transferred into an Eppendorf microcentrifuge. 30 µl of water was added and given 2 minutes to solubilise DNA before being eluted at 11,400G for one minute. DNA or RNA concentrations and purity were measured using a Nanodrop one (Thermo scientific) on the respected ratio settings 260/280 and 260/230.

2.1.4 – PCR DNA amplification

Constructs were amplified using PCR (Table 2.1.1.1). (Table 2.1.4.1) shows the volumes of each reagent of PCR reaction. (Table 2.1.4.2) shows the conditions used.

Table 2.1.4. 1 PCR reaction mixture, volumes and concentrations of reagents

Volume	Component
10 μ L	5X Phusion DNA Polymerase buffer (Thermo Scientific)
1 μ L	Phusion DNA Polymerase (Thermo Scientific, 2U/ μ l)
3 μ L	Dimethyl sulfoxide (DMSO) 100%
1 μ L	dNTPs mix (Thermo Scientific, 200mM)
1 μ L	Primer mix (250ng/ μ l)
1 μ L	DNA template (100-250ng/ μ l)
33 μ L	H ₂ O

Table 2.1.4. 2 PCR program used

Process	Temperature (°C)	Time (minutes)	Number of cycles
Initial denaturation	94	5	1
Denaturation	94	0.5	25
Annealing	60	0.5	
Extension	72	1	
Final extension	72	10	1

2.1.5 - Agarose Gel Electrophoresis

Digested vector and amplified PCR products inserts were purified on 1% and 2% agarose gels respectively. 10000X Gel Red Nucleic acid stain was added to samples with 6X laemmli loading die.

Golden gate constructs and amplified inserts were run on a 1% or 2% agarose gel, 3 μ l of SAFEView was added per 50 ml of gel. 1 μ l of 6X laemmli loading buffer was added to each 5 μ l sample. 5 μ l of 1 Kb or 100bp Gene ruler DNA ladder was loaded separately for size determination. Electrophoresis was run at 100v for 25-60 minutes and visualised using Syngene UV illuminator.

2.1.6 - Gel Extraction

DNA was purified and extracted from agarose gels using the GeneJET Gel Extraction Kit (Thermo Scientific). Obtained gel DNA segments were solubilised with 100 μ l of solubilisation buffer per 100mg of gel. Samples were heated to 55 °C for 10 minutes, and vortexed every 2 minutes. Samples were then transferred to a gel extraction column and centrifuged using Thermo Scientific minispin microcentrifuge for 1 minute at 11,400 G, discarding supernatant after the run.

Samples were then washed twice with 700 μ L of wash buffer being added to the column before each run at 11,400 G for 1 minute and then discarded. Residual ethanol was removed via an additional 2 minute spin at 11,400 G and column transferred into an Eppendorf microcentrifuge tube. DNA was solubilised for 2 minutes at RT in 30 μ L of ddH₂O before being centrifuged for 1 minute at 11,500 G.

2.1.7 - Double digests of AtS6K1 domains

To produce Kinase domain (113-408), start to kinase domain (1-408) and full length (1-465) constructs, samples are digested forming sticky ends, AtS6K1 inserts and appropriate vector were digested. Vectors pGEX-6p-1 with restriction enzymes EcoRI and XhoI, Vector pET-21 a (+) with EcoRI and nostop XhoI. Additional components for the reaction mixture are added (Table 2.1.8.1) incubated over night at 37 °C

Table 2.1.7. 1 Double digest restriction enzymes, volumes and concentrations of reagents

volume	Component
5 μ l	10X Buffer Tango
1 μ l	<i>EcoRI</i> (Thermo Scientific, 10U/ μ l)
1 μ l	<i>XhoI</i> or <i>XhoI</i> nostop (Thermo Scientific, 10U/ μ l)
30 μ l / 15 μ l	DNA insert / Vector DNA (55-180 ng/ μ l)
Make up to 50 μ l	H ₂ O

2.1.8 – Ligation of AtS6K1 constructs into pGEX-6p-1 and PET-21a (+) vector

Digested vectors and inserts were aided in ligating together with T4 DNA ligase, with insert in excess. The generated plasmids were transformed into *E.coli* DH5 α cells and plated (section 2.1.2). The colonies formed were inoculated in 10ml of LB culture with 100 μ g/ml Ampicillin and grown overnight. The amplified ligation product was purified using Plasmid Miniprep kit (section 2.1.3)

Table 2.1.8. 1 Ligation components volumes and concentrations of reagents

Volume	Component
4.3 μ l	Vector DNA (10 ng/ μ l)
3 μ l	Insert DNA (40- 50 ng/ μ l)
10 μ l	H ₂ O
2 μ l	10X T4 ligase buffer (Thermo Scientific)
1 μ l	T4 DNA ligase (Thermo Scientific)

2.1.9 - Diagnostic digest check

The DNA sample was double digested to ensure ligation and recombinant DNA formation. (Table 2.1.9.1) shows double digest components. Samples were incubated for 4 hours at 3°C and run at 100V for 45 minutes on a 1% agarose gel.

Table 2.1.9. 1 Diagnostic digest check volumes and concentrations of reagents

Volume	Component
0.5 µl	<i>EcoRI</i> (Thermo Scientific, 10U/µl)
0.5 µl	<i>XhoI</i> or nostop <i>XhoI</i> (Thermo Scientific, 10U/µl)
2 µl	Plasmid (1 µg)
1 µl	Buffer
6 µl	H ₂ O

2.1.10 - Sequence analysis

To check Purified recombinant plasmids had ligated correctly with no point mutation, samples of between 50-100 ng/ μ l were sequenced by Eurofins. This was converted into an amino acid sequence using the Expasy Translate tool (Gasteiger, 2003). The sequences were then aligned with sequences obtained from the UniProt database (UniProt, 2020) with Clustal X, a multiple sequence alignment tool (Larkin et al., 2007).

2.2 – Protein work

2.2.1 – Test expression

2 ml of the transformed BL21 cell culture (from protocol 2.1.2) was added to 50 ml of LB with 100 μ g/ml of antibiotic. Samples were incubated for an hour with shaking and induced with 60 ng/ml when optical density (OD) was recorded between 0.5 – 0.6 with Nano drop one (Thermo scientific) spectrophotometer at A280 setting. 2 ml of culture pre-induction and 3 hrs post induction were collected and spun for 10 minutes at 4000 RPM. The supernatant was discarded and the pellet resuspended in 25 μ l of Pbs before adding 25 μ l of 2x Laemmeli loading die. Samples were then boiled for 30 minutes. 15 μ l of DNase was mixed with samples before being centrifuged for 15 minutes at 13.4000 RPM and the supernatant run and visualised on an SDS - PAGE gel.

2.2.2 – SDS Page

Proteins were identified on a 12% SDS-PAGE electrophoresis gel (Table 2.2.2.1), running at 200 V for 50 minutes in SDS-PAGE running buffer (Table 2.2.2.1). 4 μ l of Thermofisher Prestained Protein PageRuler Ladder was added to one well and 4 μ l

loaded of sample plus Laemmli. The SDS-PAGE Gels proteins were stained using SimplyBlue™ SafeStain. The gels were submerged in the stain for 1-2 hr followed by two wash stages in water, 1-3 hr followed by an additional 1 hr wash.

Table 2.2.2. 1 SDS-PAGE gel volumes and concentrations of reagents

Reagent	Components
SDS-PAGE gel 12%	<p>Per gel</p> <p>Resolving gel: 1.6 mL of ddH₂O, 2 ml of Acrylamide/Bis-acrylamide 30 % solution, 1.3 ml of 1.5 M Tris/HCl at pH 8.8, and 50 µl of 10 % SDS. Prior to pouring 50 µl of 10 % APS is added with 5 µl N,N,N',N'Tetramethylethylenediamine (TEMED)</p> <p>Additionally stacking gel is then added: 1.5 ml of ddH₂O, 335 µl of Acrylamide/Bis-acrylamide 30 % solution, 625 µl of 0.5 M Tris/HCl at pH 8.8, and 50 µl of 10 % SDS. Prior to pouring 50 µl of 10 % APS is added with 5 µl N,N,N',N'Tetramethylethylenediamine (TEMED)</p>
SDS-PAGE running buffer	<p>14.45 g of Glycine (0.2 M, Fisher Scientific), 3 g of Tris base (25 mM, Fisher Scientific) and 0.5 g of SDS (0.05 %, Fisher Scientific) and was dissolved in ddH₂O up to 1l</p>

2.2.3 – Expression

10 ml of transformed BL21 cell culture was added to room temperature (RT) autoclaved auto-induction media (table 2.2.3.1). Cells were grown in 100 µg/ml Ampicillin, 5 ml of 99.8% glycerol and incubated at 37 °C for 3hr then 18 °C overnight.

Table 2.2.3. 1 Expression media volumes and concentrations of reagents

Volume	Component
1L	Dd H ₂ O
5 ml	Glycerol 99.8%
3.85g	Auto-induction media

2.2.4 – protein purification

Cell cultures were centrifuged for 15 minutes at 4 °C and 4000 RPM. The supernatant was discarded and the pellet re-suspended in phosphate-buffered saline (PBS) for storage at -80. For purification, the pellet was re-suspended in lysis buffer (Table 2.2.4.1) and stirred on ice. The cells were lysed using an emulsiflex at 10000 - 15000 psi, repeating through twice. The lysate was centrifuge for 45 minutes at 4 °C at 17000 RPM. Affinity chromatography was used to separate target protein from cell contents. The HIS tag column was calibrated with wash buffer (Table 2.2.4.1) prior to the loading of the supernatant and further cleaned with wash buffer (Table 2.2.4.1). The HIS tag column bound protein was collected with the elution buffer (Table 2.2.4.1) from the competitive binding of imidazole added 1.03g per 50 ml. For glutathione-s-transferase (GST) tagged protein separation, a GST tag column was used and calibrated with wash buffer (Table 2.2.4.2) prior to the loading of supernatant fraction and cleaned with wash buffer (Table 2.2.4.2). The GST tag bound protein was collected with the elution buffer (Table 2.2.4.2) from the competitive binding of 50 mM glutathione.

Table 2.2.4. 1 HIS tag protein purification buffers volumes and concentrations of reagents

Reagent	Components
Wash Buffer (250ml)	50mM Tris pH 7.5 (12.5 ml of 1 M), 300 mM NaCl (15 ml of 5 M), 5% glycerol (912.5 ml), 0.01% Triton X (250 μ l of 10%), 1 mM MgCl ₂ (0.5 ml of 0.5M), 0.5 mM ATP (1.25 ml of 100 mM), ddH ₂ O (208 ml)
Lysis Buffer	Wash buffer (100 ml), protease inhibitor tablet, 200 μ l of DNase
Elution Buffer	Wash buffer (50 ml), 1.02g imidazole

Table 2.2.4. 2 GST tag protein purification buffers volumes and concentrations of reagents

Reagent	Components
Wash Buffer (250ml)	50mM Tris pH 7.5 (12.5 ml of 1 M), 300 mM NaCl (15 ml of 5 M), 5% glycerol (912.5 ml), 0.01% Triton X (250 μ l of 10%), 0.01% Triton X (250 μ l of 10%), 1 mM MgCl ₂ (0.5 ml of 0.5M), 0.5 mM ATP (1.25 ml of 100 mM), 5mM β -Mercaptoethanol (87 μ l of 14.3M) and 0.5 mM EDTA (1.25 ml of 100 mM)
Lysis Buffer	100 ml of wash buffer with 200 μ l of DNase
Elution Buffer	20 ml of wash buffer with 10 mM Glutathione (0.154g in 50 ml)

2.3 – Golden gate cloning

2.3.1 – Golden gate primer design

Golden gate primers were designed on SnapGene with (protocol 2.1.1) and obtained from Sigma-Aldrich (Appendix A-F). Using the online tool (T_m Calculator) the GC% and T_m values were determined. Forward primers are indicated by (F) and reverse primers are indicated by (R).

Table 2.3.1. 1 Primer properties used for PCR of golden gate inserts

Primer	length	Tm (°C)	GC %	Sequence (5'-3')
clo_S6K1_F	22	65	45.4	TGTGGTCTCAAATGGTTTCCTC
clo_S6K1_R	38	79	50	CGTGGTCTCAAAGCCTACAAAGTAGTTGTG GACTGGTG
clo_S6K1pro(s))_F	19	61.8	57.8	TGTGGTCTCAGGAGTCAGC
clo_S6K1pro(s))_R	35	79.8	45.7	CCGTGGTCTCAATGGAATTTACACGGGAAA AATCG
Clo_S6K1pro(B)_F	20	65.2	55	TGTGGTCTCAGGAGGAATGG
Clo_CDS_GF P_F	28	62	61	TGTGGTCTCACCATGGTGAGCAAGGGCG
Clo_CDS- mCherry_R	20	62.1	50	CGTGGTCTCAAAGCTCACTT

2.3.2 – DNA insert PCR amplification

Plasmids containing Inserts were provided by ThermoFisher and amplified using PCR primers (Table 2.3.2.1) for each insert (Table 2.3.2.1). (Table 2.3.2.2) shows the volumes of each reagent of PCR reaction and (Table 2.3.2.3) shows the conditions used. PCR clean-up was then performed with (protocol 2.1.3).

Table 2.3.2. 1 Primer for insert amplification

Plasmid	Primer 1	Primer 2	Insert produced
S6K1pro (small) +pUC57-KANA	clo_S6K1pro(s)_F	clo_S6K1pro(s)_R	S6k1pro(small)_Amplified
S6K1pro (Big) +pUC57-KANA	clo_S6K1pro(B)_F	clo_S6K1pro(s)_R	S6k1pro(Big)_Amplified
S6K1 +pUC57-KANA	clo_S6K1_F	clo_S6K1_R	S6K1_Amplified
pICSL80007 (CDS_mCherry)	Clo_CDS-GFP_F	Clo_CDS-mCherry_R	CDS-mCherry_Amplified

Table 2.3.2. 2 PCR reaction mixture, volumes and concentrations of reagents

Volume	Component
10 μ L	5X Phusion DNA Polymerase buffer (Thermo Scientific)
0.5 μ L	Phusion DNA Polymerase (Thermo Scientific, 2U/ μ l)
1 μ L	dNTPs mix (Thermo Scientific, 200mM)
1 μ L	Primer (F) (250ng/ μ l)
1 μ L	Primer (R) (250ng/ μ l)
1 μ L	DNA template (100-250ng/ μ l)
35.5 μ L	H ₂ O

Table 2.3.2. 3 PCR program used

Process	Temperature (°C)	Time (minutes.seconds)	Number of cycles
Initial denaturation	98	0.30	1
Denaturation	98	0.10	35
Annealing	60	0.15	
Extension	72	2.30	
Final extension	72	5.0	1

2.3.3 – Golden gate protocol

Plasmid constructs were generated using the Golden gate reaction. (Table 2.3.3.1) shows the components and volumes of each reagent in the reaction. For each construct, 9 μL of the golden gate reaction mixture was added to 2 μL of each insert (Table 2.3.3.2) and made up to 15 μL . (Table 2.3.3.3) shows the conditions of reaction used. 35S_(double)_amplified was provided by post-Doc. PICSL30003 (NT_mCherry) were obtained from post-Doc cell culture via mini Prep (protocol 2.1.3).

Table 2.3.3. 1 Golden gate reaction mixture, volumes and concentrations of reagents

Volume	Component
2 μ L	Terminator NOS
1 μ L	Lvl 1 acceptor
1.5 μ L	T4 DNA ligase buffer
1.5 μ L	BSA
0.5 μ L	BSAI enzyme
0.5 μ L	T4 DNA ligase enzyme
2 μ L	Insert 1
2 μ L	Insert 2
2 μ L	Insert 3 or H ₂ O
2 μ L	H ₂ O

Table 2.3.3. 2 Golden gate constructs insert combination

n.o	Construct	Insert 1	Insert 2	Insert 3
1	S6K1pro(S)_mCherry_S6K1	S6k1pro(small)_Amplified	PICSL30003 (NT_mCherry)	S6K1_Amplified
2	S6K1pro(B)_mCherry_S6K1	S6k1pro(Big)_Amplified	PICSL30003 (NT_mCherry)	S6K1_Amplified
3	35S-mCherry-S6K1	35S_(double)_Amplified	PICSL30003 (NT_mCherry)	S6K1_Amplified
4	35S-mCherry	35S_(double)_Amplified	CDS-mCherry_Amplified	H ₂ O
5	S6K1pro(B)_mCherry	S6k1pro(Big)_Amplified	CDS-mCherry_Amplified	H ₂ O
6	S6K1pro(s)_mCherry	S6k1pro(Smal)_Amplified	CDS-mCherry_Amplified	H ₂ O

Table 2.3.3. 3 Golden gate program used

Process	Temperature (°C)	Time (minutes.seconds)	Number of cycles
Activation of restriction enzyme	37	0.20	1
Activation of restriction enzyme	37	3.0	26
Activation of ligase	16	4.0	
Inactivation of enzyme	50	5.0	1
Inactivation of ligase	80	5.0	1
Hold	16	-	1

2.3.4 - Blue white screening

Generated plasmids were transformed into E.Coli top 10 cell line with (protocol 2.1.2) and plated for blue white screening. Colonies displaying white phenotype with antibiotic resistance for successful golden gate plasmid formation were picked and diluted in 5 μ l of H₂O.

2.3.5 – Colony PCR

2 μ l of diluted transformed E.Coli top 10 cells insert sequences were amplified using primer properties and combinations respectively (Table 2.3.5.1) (Table 2.3.5.2). GC% and T_m value were calculated using an online tool (T_m Calculator). Forward primers are indicated by (F) and reverse primers are indicated by (R). (Table 2.3.5.3) shows the volumes of each reagent for PCR reaction. (Table 2.3.5.4) shows the conditions used.

Table 2.3.5. 1 Primer properties used for colony PCR of constructs

Primer	length	Tm (°C)	GC%	Sequence (5'-3')
Seq-plim – R – F	21	58	52	CGGATAAACCTTTTCACGCC
Clo-35s-double R	36	53	36	CGTGGTCTCAATGGGTATCGATAAT TGAAATGTAA
Clo-S6K1pro(s)-R	35	53	46	CCGTGGTCTCAATGGAATTTACACG GGAAAAATCG

Table 2.3.5. 2 Primer combination selected for colony PCR of target constructs

n.o	Construct	Primer 1 (F)	Primer 2 (R)
1	S6K1pro(S)_mCherry_S6K1	Seq-plim – R – F	Clo-S6K1pro(s)-R
2	S6K1pro(B)_mCherry_S6K1	Seq-plim – R – F	Clo-S6K1pro(s)-R
3	35S-mCherry-S6K1	Seq-plim – R – F	Clo-35s-double R
4	35S-mCherry	Seq-plim – R – F	Clo-35s-double R
5	S6K1pro(B)_mCherry	Seq-plim – R – F	Clo-S6K1pro(s)-R
6	S6K1pro(s)_mCherry	Seq-plim – R – F	Clo-S6K1pro(s)-R

Table 2.3.5. 3 Colony PCR reaction mixture, volumes and concentrations of reagents

Volume	Component
1.5 μ L	Taq buffer (Thermo Scientific)
0.15 μ L	Taq DNA Polymerase (Thermo Scientific)
0.3 μ L	dNTPs mix (Thermo Scientific, 200mM)
0.3 μ L	Primer 1 (F) (250ng/ μ l)
0.3 μ L	Primer 2 (R) (250ng/ μ l)
2 μ L	DNA template (100-250ng/ μ l)
10.45 μ L	H ₂ O

Table 2.3.5. 4 Colony PCR program used

Process	Temperature (°C)	Time (minutes.seconds)	Number of cycles
Initial denaturation	94	3.0	1
Denaturation	94	0.15	35
Annealing	55	0.20	
Extension	72	2.05	
Final extension	72	10.0	1

2.3.6 – Plant growth

Arabidopsis ecotype Col-0 and its transgenic variants seeds were planted in soil. After germination, the luminosity was scheduled in 8 h/16 h light-dark cycles at 21 °C and relative humidity of 65 % before being transplanted into separate pots after 2 weeks. The plant environment was kept constant in well-watered control conditions.

2.4 – RNA Sequencing

2.4.1 – RNA-Seq short reads processing

Short reads files were obtained in FastQ format and assessed using the FastQC tool which is a quality control tool used to check obtained reads from high throughput sequencing pipelines. A graphical interface identifies various modular analyses such as per base sequence quality and per base sequence content.

(<https://www.bioinformatics.babraham.ac.uk/projects/fastqc/>). Sequenced reads were aligned to the TAIR10 *Arabidopsis* genome

(https://www.Arabidopsis.org/download/indexauto.jsp?dir=%2Fdownload_files%2FGenes%2FTAIR10_genome_release). HISAT2 tool program was used for a fast and sensitive spliced alignment, mapping RNA-seq reads to the reference genome by small Hierarchical Graph FM indexes (HGFM) that cover the whole genome (Kim et al., 2019). Resultant reads were analysed with the tool Kallisto, performing a pseudo-alignment approach to quantify transcript presence (Bray, Pimentel, Melsted and Pachter, 2016).

2.4.2 – Differential expression analysis

The output file from Kallisto was analyzed for differential expression utilising the *Arabidopsis* TAIR10 genome obtained from www.Arabidopsis.org and the quantification file were fed into the 3D RNA-Seq pipeline (Guo et al., 2020; Calixto et al., 2018). The RNA-seq data had 2 factor groups: wild type no stress (WTNS) and wild type heat stress (WTHS). Each factor contained 4 biological replicates producing a total of 8 samples. Transcript per million reads (TPMs) and counts were generated using tximport R package version 1.10.0. lengthScaledTPM method inputs transcript quantifications from command line Kallisto tool (Bray, Pimentel, Melsted and Pachter, 2016). Low expressed genes and transcripts were filtered by analysing the data mean-variance trend. The decreasing trend between data mean and variance was observed when expressed transcripts were classed as those which had ≥ 1 of the 16 samples with count per million reads (CPM) ≥ 1 , providing an optimised filter of low expression. The identification of expressed genes was determined by transcripts fitting the above criteria. To normalise the gene and transcript read counts the trimmed mean of M values method (TMM) was used to produce \log_2 -CPM (Guo et al., 2020; Calixto et al., 2018). A principal component analysis (PCA) plot was used to determine the presence of batch effects in the data set, employing orthogonal transformation to convert a list of observations of possibly correlated variables.

Limma R package was used to compare the expression changes between conditions of experimental design balancing the outliers from potential degradation or contamination. The \log_2 fold change (L2FC) of gene/transcript abundance were calculated for groups WTHS-WTNS. To test the significance of expression changes a t-test carried out. P-values adjustments for multiple testing with Benjamini-

Hochberg value (BH) were made to correct the false discovery rate (FDR) (Guo et al., 2020; Calixto et al., 2018). Significantly differentially expressed genes in a contrast group would be identified if it had adjusted p-value < 0.01 and L2FC ≥ 1 . Additionally, hierarchical clustering partitioned the DE genes into 10 clusters with euclidean distance and average clustering algorithm. Heat maps were generated with Complex heatmap R package version 1.20.0. Venn diagrams enabled the interpretation of results and comparison between known TOR related genes and DE genes.

Chapter 3 - Results

3.1 - Cloning of AtS6K1 constructs

The successful purification of S6K1 is yet to be seen and thus it would be of great importance being the first to do so, enabling the determination of biochemical roles and aid in solving the 3D crystal structure of AtS6K1. This study aims to fill the gap in the research, with the cloning and expression of recombinant AtS6K1 protein.

The AtS6K1 constructs were amplified using PCR and further isolated with agarose gel electrophoresis. The three bands produced were visible between 750bp and 1500bp which is the correct expected size region (Fig 3.1A). The gene inserts were then extracted and along with vector DNA digested with their respective restriction enzymes. The digested vector was purified by running on a 1% agarose gel isolating the linear digest, causing it to run above the undigested vector (Fig 3.1 B, C). The DNA was then extracted using a gel extraction kit and Qiagen's PCR purification kit for the digested insert DNA. The sticky ends generated through the digest enables ligation of vector to each insert. The sequences were then confirmed via sanger-sequencing, aligning with obtained sequence to ensure no mutations were present (Appendix G-I).

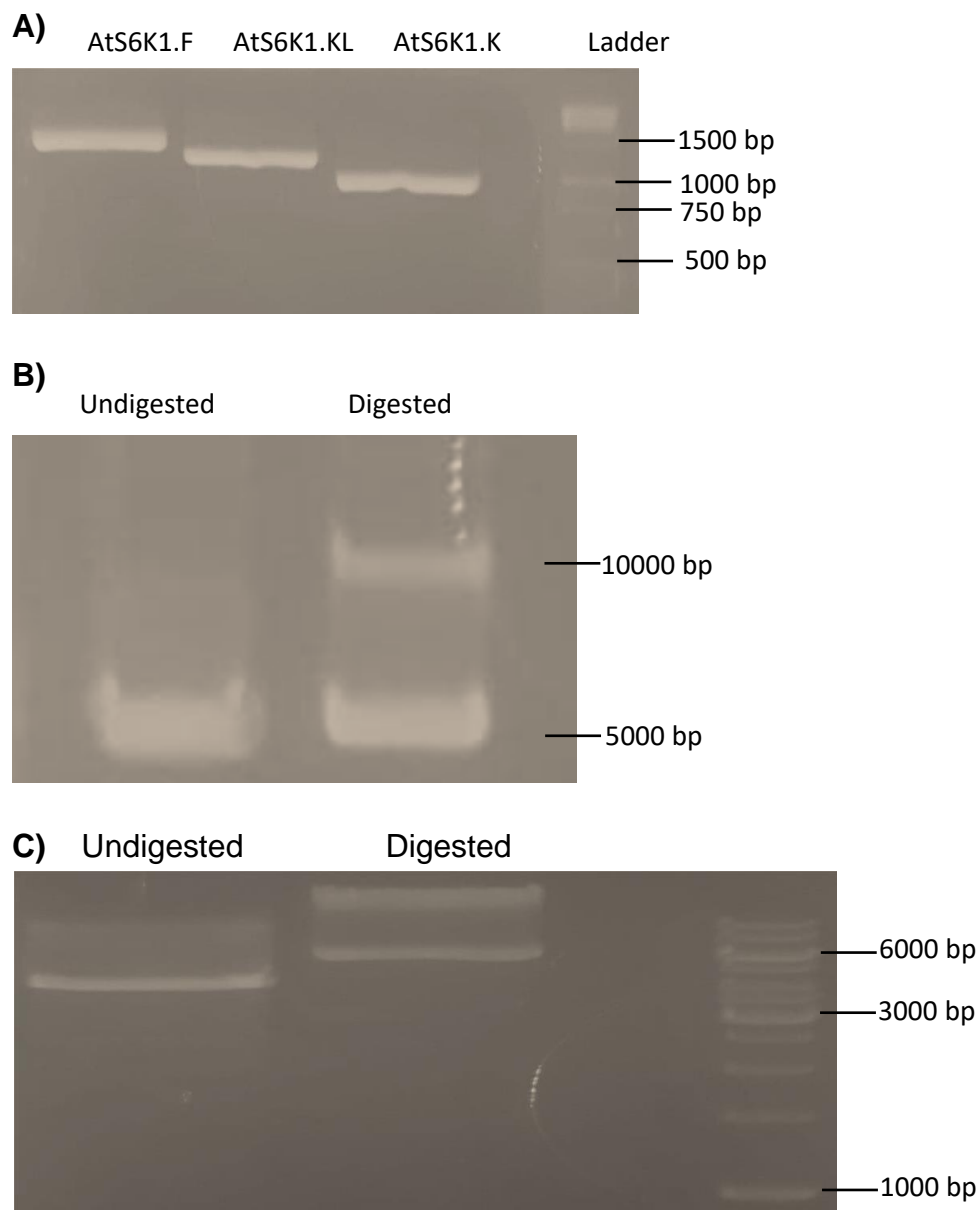


Figure 3. 1. Cloning of AtS6K1 constructs into vectors

A) Agarose gel electrophoresis of AtS6K1 domains. AtS6K1 full length (F) (1-465), Kinase long (KL) (113-465), or kinase domain (K) (113-408) domains were amplified with PCR and visualised on 2% agarose gel via electrophoresis. Loading dye was added prior to electrophoresis run at 100V for 40 minutes. The gel was visualised on a Syngene illuminator and photographed using a mobile phone camera. **B)** Agarose gel electrophoresis of undigested and linear digest pGEX-6p-1 vector. Digested vector was purified on 1% agarose gel electrophoresis. Loading dye was added before electrophoresis run at 100V for 25 minutes. The gel was visualised on a Syngene illuminator and photographed using a mobile phone camera. **C)** Agarose gel electrophoresis of undigested and linear digest Pet-21a (+) vector. Digested vector was purified on 1% agarose gel electrophoresis. Loading dye was added prior to electrophoresis run at 100V for 25 minutes. The gel was visualised on a Syngene illuminator and photographed using a mobile phone camera.

3.2 - Protein expression of GST tagged AtS6K1 protein

After conformation of tagged AtS6K1 plasmids constructs, samples were transformed into BL21 cell lines due to the high efficiency of competent cells for protein expression under a T7 promoter. Test expression was induced with 0.5mM IPTG and acceptable levels for inducing in a pGEX vector. This was done when an optical density (OD₆₀₀) between 0.5-0.6 was reached, due to cells being in their exponential growth stage. Extracted samples were stained and visualised via sodium dodecyl sulphate–polyacrylamide gel electrophoresis (SDS-Page). AtS6K1 F, KL, K should be visualised at 79.4 KDa, 66.4 KDa and 60.1 KDa respectively. A band was visualised for all induced constructs in the 26 KDa range however not in the expected (Fig 3.2A). Test expression was further repeated giving the same result (Fig 3.2A). Expression and purification of the full protein construct was carried out to distinguish between potential bands, producing bands in the 26KDa region (Fig 3.2B). Autoinduction media was used as it proven to be more effective for protein expression. This was further repeated with the Kinase to end of protein sequence again giving bands in the 26 KDa region (Fig 3.2B).

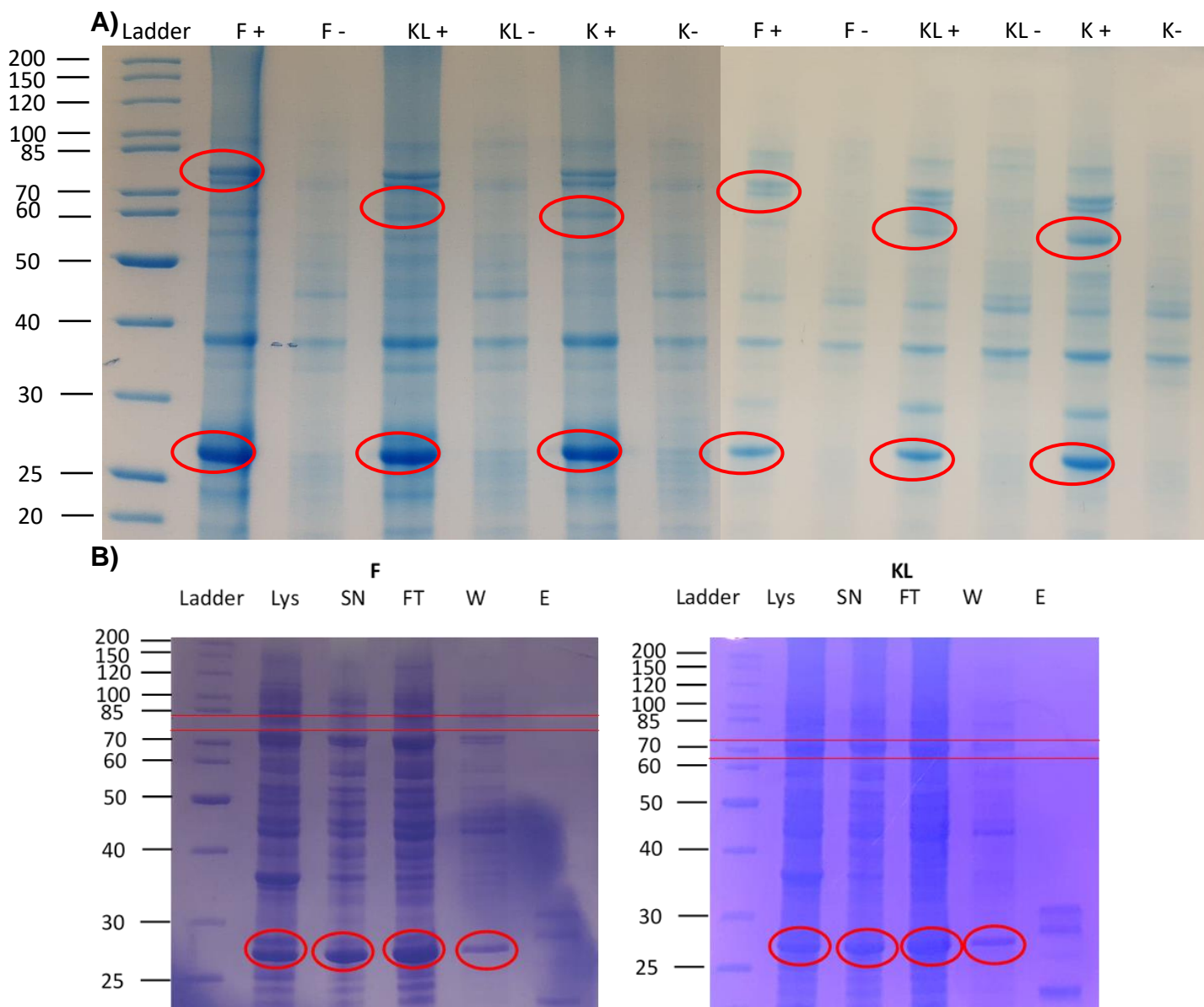


Figure 3. 2 Protein expression of GST tagged AtS6K1 protein

A) Test expression and a repeat of construct in pGEX-6p-1 vector in BL21 cells were run on a 12% SDS-PAGE. Loading dye was added to sample and boiled on and off for 10 minutes prior to electrophoresis. SDS-page was run at 200V for 50 minutes. The gels were stained with SimplyBlue™ SafeStain and destained in water prior to being Photographed, using a mobile phone camera. (+) represents induced and (-) non-induced expression. (F) full length construct, (KL) kinase long construct and (K) kinase domain. The red circles highlight expected or identified protein. B) The purification of F and KL fractions in pGEX-6p-1 vector run on a 12% SDS-PAGE. Loading dye was added to sample and boiled on and off for 10 minutes prior to electrophoresis. SDS-PAGE was run at 200V for 50 minutes. The gels were stained with SimplyBlue™ SafeStain and destained in water prior to being Photographed, using a mobile phone camera. (Lys) represents cell lysate, (SN) centrifuged supernatant, (FT) flow through, (W) wash buffer and (E) elution buffer. The red bands represent the expected protein region and red circles show suspected proteins.

3.3 - Protein expression of HIS tagged AtS6K1 protein

AtS6K1 kinase domain (K) and Kinase to end (KL) proteins with a C terminal HIS tagged were transformed into BL21 cells for their high protein expression levels under the T7 promotor. Test expression was induced with 0.5mM IPTG for effective induction in a Pet-21a (+) vector. Samples were stained before visualising on SDS-Page (Figure 3.3A). AtS6K1 F, KL, K should be visualised at 55.1 KDa, 41.9 KDa and 35.6 KDa respectively. This was further repeated for the KL sequence in BL21 and an additional BL21 derivative (Rosetta) cell line (Figure 3.3B). Expression of C-terminal His-tagged KL was carried out followed by purification, staining and visualisation via SDS-Page (Figure 3.3C). This didn't produce any bands in expected regions, with some fainter bands seen are likely to be common cellular proteins.

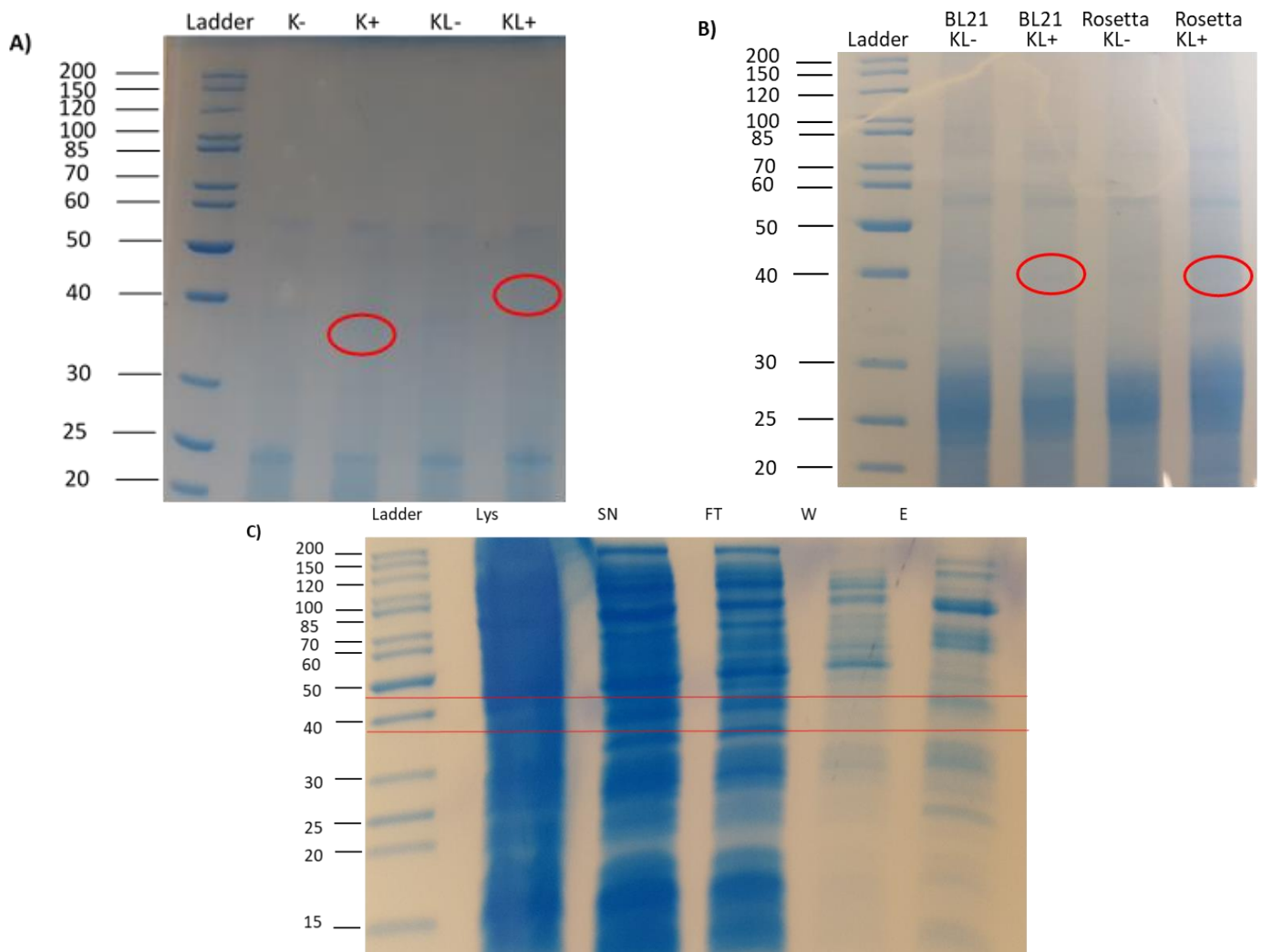


Figure 3.3 Protein expression of HIS tagged AtS6K1 protein

A) Test expression of K un, K induced, KL un, KL induced BL21 via Pet-21a (+) vectors run on a 12% SDS-PAGE. Loading dye was added to sample and boiled on and off for 10 minutes prior to electrophoresis. SDS-page was run at 200V for 50 minutes. The gels were stained with SimplyBlue™ SafeStain and destained in water prior to being Photographed, using a mobile phone camera. (+) represents induced and (–) non-induced expression. (KL) depicts kinase long construct and (K) kinase domain. The red circles represent expected protein by size. **B)** Test expression of KL in BL21 and ROSS cell line via Pet-21a (+) vectors run on a 12% SDS-PAGE. Loading dye was added to sample and boiled on and off for 10 minutes prior to electrophoresis. SDS-page was run at 200V for 50 minutes. The gels were stained with SimplyBlue™ SafeStain and destained in water prior to being Photographed, using a mobile phone camera. (+) represents induced and (–) non-induced expression. (KL) depicts kinase long construct and (K) kinase domain. The red circles represent expected protein by size. **C)** Fractions through Expression and purification KL in Pet-21a (+) vector were run on a 12% SDS-PAGE. Loading dye was added to sample and boiled on and off for 10 minutes prior to electrophoresis. SDS-page was run at 200V for 50 minutes. The gels were stained with SimplyBlue™ SafeStain and destained in water prior to being Photographed, using a mobile phone camera. (Lys) represents cell lysate, (SN) centrifuged supernatant, (FT) flow through, (W) wash buffer and (E) elution buffer. The red bands represent the expected protein region.

3.4 - Plant gene construction

Cellular localisation and expression of AtS6K1 was clarified with the addition of monomeric red fluorescent protein tagged to AtS6K1 with native promoter or over expressed 35S promoter via golden gate cloning. Amplification of 4 insert sequences from provided plasmids was carried out for level 0 section and was visualised in the expected region under agarose gel electrophoresis (Fig 3.4A). S6K1proSMALL 1287 bp, S6K1proBIG 1878 bp, S6K1 1423 bp, CDS-Mcherry 737 bp Golden gate cloning, transformation with blue-white screening, colony PCR and visualisation under agarose gel electrophoresis gave bands in the expected region of sections of the construct (Fig 3.4B-D).

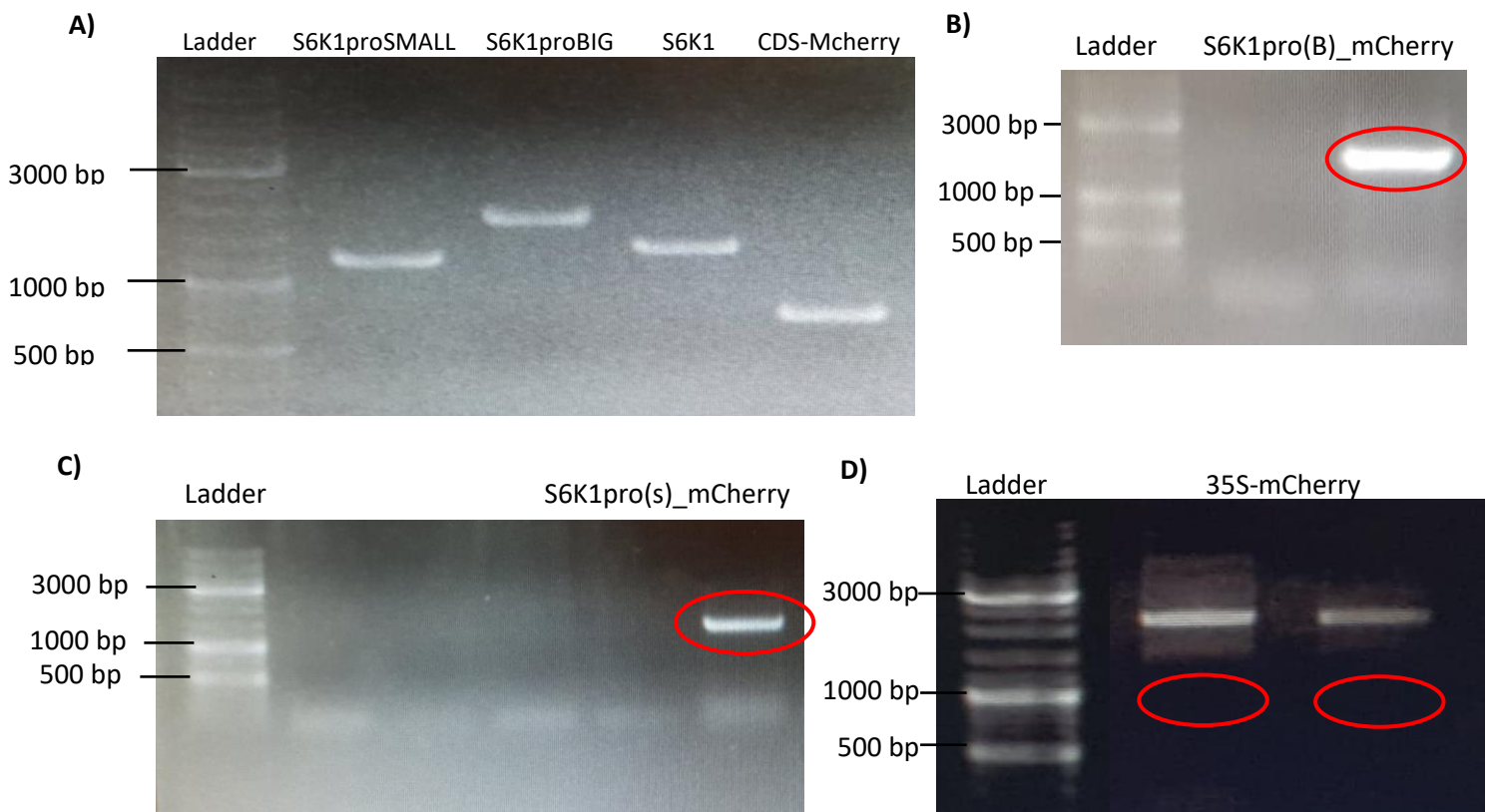


Figure 3. 4 Gene construction for plant vectors

A) Amplification of 4 insert sequences, S6K1proSMALL, S6K1proBIG, S6K1, CDS-Mcherry purified on 1% agarose gel electrophoresis. Loading dye was added prior to electrophoresis run at 100V for 25 minutes. The gel was visualised on a Syngene illuminator and photographed using a mobile phone camera. **B)** Colony PCR construct discovery of S6K1pro(B)_mCherry purified on 1% agarose gel electrophoresis. Loading dye was added prior to electrophoresis run at 100V for 25 minutes. The gel was visualised on a Syngene illuminator and photographed using a mobile phone camera. The red circle highlights the expected construct at 1998 bp. **C)** Colony PCR construct discovery S6K1pro(s)_mCherry purified on 1% agarose gel electrophoresis. Loading dye was added prior to electrophoresis run at 100V for 25 minutes. The gel was visualised on a Syngene illuminator and photographed using a mobile phone camera. The red circle highlights the expected construct at 1998 bp. **D)** Colony PCR construct discovery 35S-mCherry purified on 1% agarose gel electrophoresis. Loading dye was added prior to electrophoresis run at 100V for 25 minutes. Gel was visualised on a Syngene illuminator and photographed using a mobile phone camera. The red circle highlights the expected construct at 977 bp.

3.5.1 - RNA Sequencing output of heat stress *Arabidopsis thaliana*

Gene expression profiles available from public datasets (Kilian et al., 2007) has shown that expression levels of AtS6K1 can be influenced under different abiotic stresses (Fig 3.5.1). Analysis of this data showed that AtS6K1 had increased expression levels under heat stress conditions in both shoot and root tissues. We therefore analysed a heat stress RNA sequencing dataset to generate a more detailed transcriptomic view of TOR regulated genes under stress conditions.

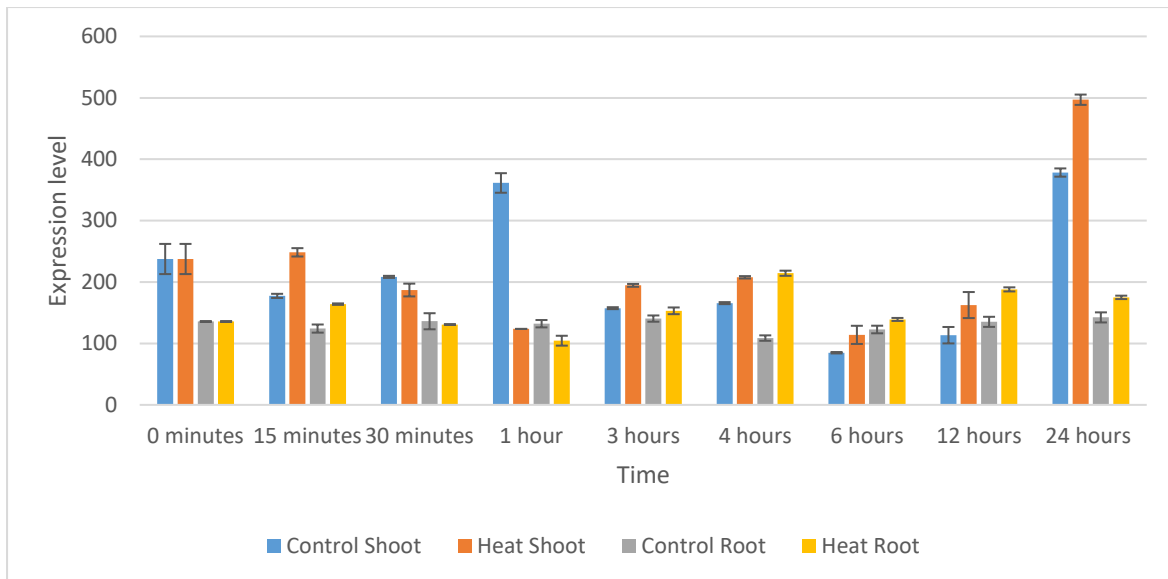


Figure 3.5. 1 Increased expression of AtS6K1 Gene Chip in *Arabidopsis*

Expression levels of AtS6K1 in roots and shoots at different time interval under heat stress. Stress treatment on 16 day old plants started at 3 hours of light subjecting to 38°C. Samples taken at 0.25, 0.5, 1.0, 3.0h of hs and +1, +3, +9, +21h recovery at 25°C).

S6K1 function has been linked to stress responses in plants but its exact function under heat stress is unknown. The complete de-phosphorylation of rpS6 in tomato cell cultures was seen in parallel with heat stress, suggesting heat stress-specific involvement of S6k1 (Scharf and Nover, 1982). S6K1 related transcription factors were therefore targeted for potentially being differentially expressed in these conditions.

The identification of differentially expressed genes from WT Col-0 plants under heat stress at 37°C for 30 mins were used. This was due to the influence in AtS6K1 expression shown at 30 mins in the public datasets (Kilian et al., 2007). Kallisto was used to quantify transcript abundances in RNA-Seq experiments (Bray, Pimentel, Melsted and Pachter, 2016). Transcript abundance was then subsequently used to determine DEGs before filtered in the 3DNAseq app (Guo et al., 2020; Calixto et al., 2018). This generated 3919 differentially expressed genes that were identified (Fig 3.5.2) and clustered according to expression profiles under heat stress in WT. Genes were divided into 10 distinct clusters expression were visualised (Figure 3.5.2). Of the 3919 DE genes 1804 were up-regulated and 2115 were down-regulated (Fig 3.5.3) with low expression transcripts being removed (Fig 3.5.4). The heat stress-related response to both AtS6K1 and AtS6K2 was searched for in the TPM generated and plotted to reveal a kinase-specific response (Fig 3.5.5). This showed that AtS6K1 was regulated by heat stress as expected (Kilian et al., 2007), being significantly down-regulated. However, no response was seen for AtS6K2 in this novel test, confining AtS6K2 to salt stress regulation (Winter et al., 2007).

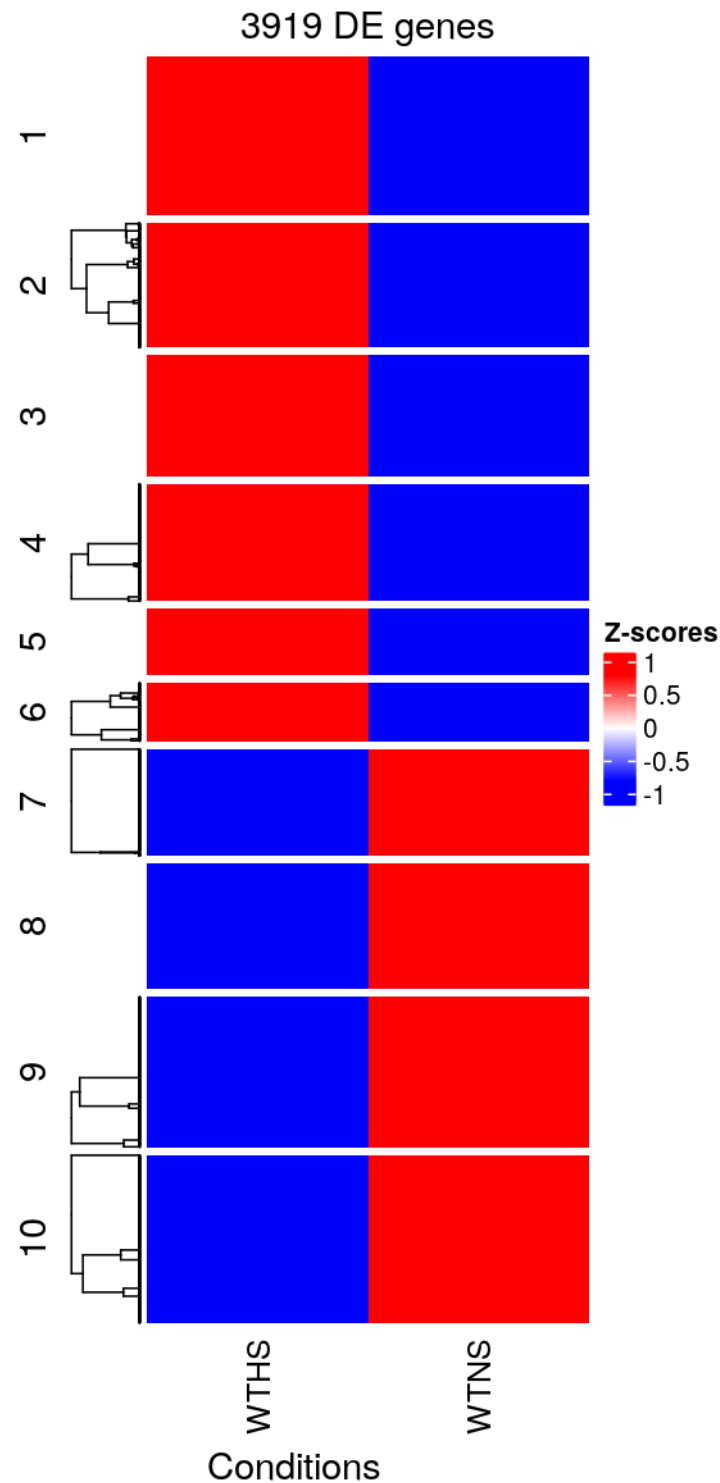


Figure 3.5. 2 Heat map depiction of changes in expression for target groups

Cluster analysis of identified 3919 Differentially expressed (DE) genes from 2 target groups WTHS and WTNS. Hierarchical clustering divided the DE genes into 10 clusters with euclidean distance and average clustering algorithm. Heat maps generated with Complex heatmap R package version 1.20.0.

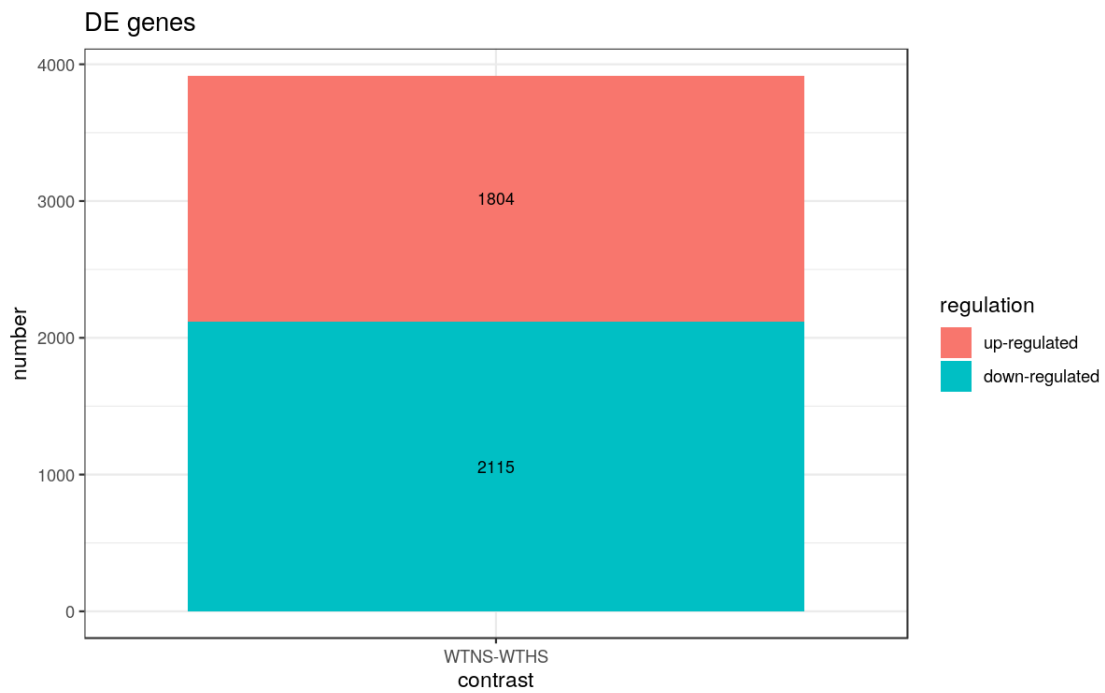


Figure 3.5. 3 Number of up and down-regulated genes

The numbers are calculated based on positive or negative signs on the L2FC of DE genes

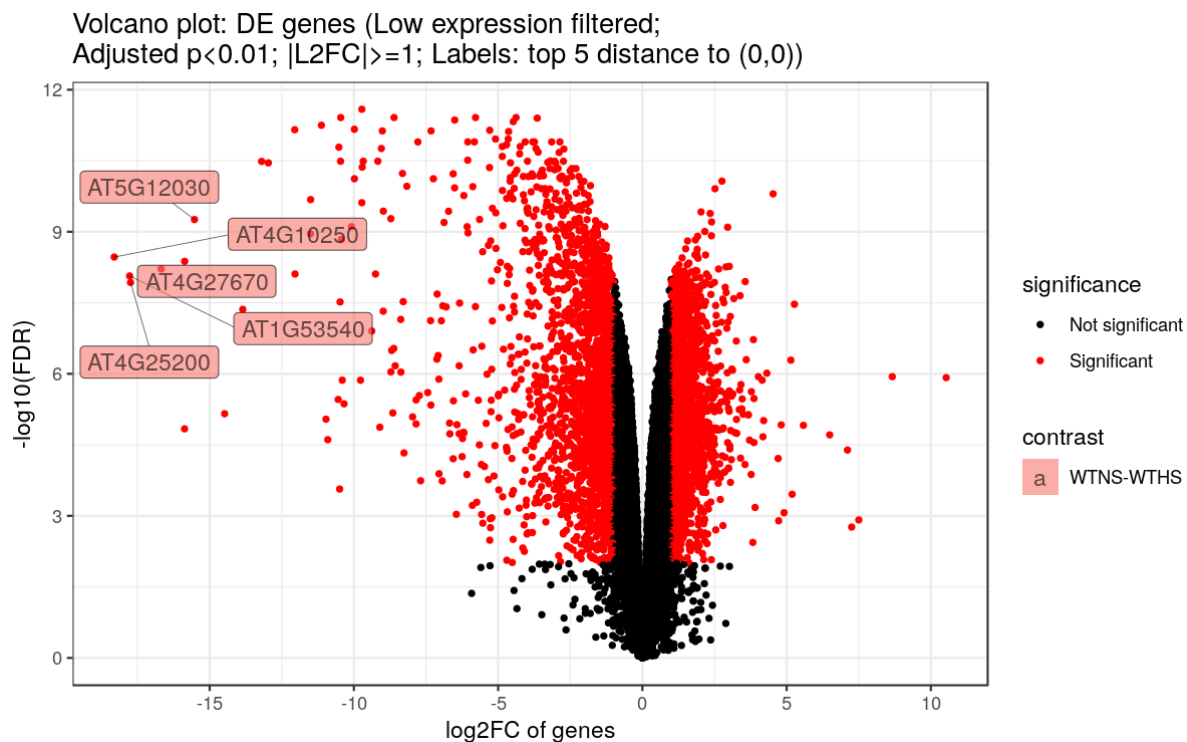


Figure 3.5. 4 Volcano plot highlighting significant genes in contrast groups

The vertical axis (y-axis) corresponds to the Significantly DE gene with an adjusted p-value of < 0.01 and $-\log_{10}(\text{FDR})$ (false discovery rate) of 2. The horizontal axis (x-axis) displaying the log 2 fold change value $L2FC \geq 1$. Positive x-values represent up-regulated genes. Negative x-values represent down-regulated genes.

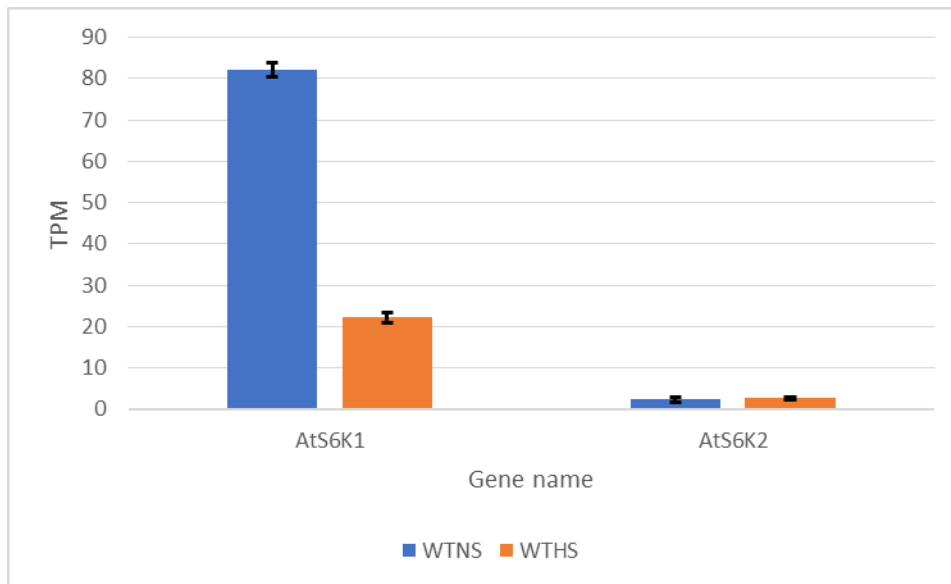


Figure 3.5. 5 Down-regulation of AtS6K1 transcripts

The mean TPM expression values of genes from 4 replicates corresponding to the vertical axis (y-axis) for different kinases comparing heat stress (HS) to no stress (NS) control. Standard errors determined by the standard deviation of samples divided by the square root of sample size.

3.5.2 - Overlapping gene identification experiment

Due to S6K1 expression being altered by heat stress, we searched for the presence of known TOR regulated and known S6K transcription factor target genes (Fig 1.2). The TOR target protein IDs identified from pull-down assays (Van Leene et al., 2019), were mapped to the *Arabidopsis* database Araport and converted to their gene name for comparison (Van Leene et al., 2019). Similarly, known downstream S6K transcription factors E2F, ABA and RBR1 related genes were obtained for overlapping analysis to establish whether specific TF were targeted in response to heat stress (Fig 3.5.6).

ABA-responsive genes including abiotic stress adaption genes *Em1*, *Em6*, and *RAB18* was significantly upregulated in seedlings over-expressing *AtS6K2* when treated with ABA and AZD (Li et al., 2021). Additionally, BIN2 a negative regulator of brassinosteroid signalling plays a role in interacting with ABI5 to mediate BR and ABA signalling during abiotic stress and seed germination (Skubacz et al., 2016). BIN2 phosphorylates ABI5 stabilising it to mediate ABA (Skubacz et al., 2016). Additionally, a recent interaction was seen between *AtS6K2* and *AtABI5*, positively modulating ABA responses during seedling growth (Li et al., 2021). This suggests a direct interaction between ABA signalling pathways and TOR. Stress induced target genes of ABI5 were therefore selected (Skubacz et al., 2016).

The top best 200 E2Fa-bound genes identified by ChIP, Tandem Chromatin Affinity Purification (TChAP) and Chromatin Affinity Purification (ChAP) published by

(Verkest et al., 2014). RBR1 genes upregulated at least once in 32 compiled stress experiments covering all biotic, abiotic stresses, infrared, High energy or gamma radiation Stress experiments, in comparison with RBR1-bound genes were used (Bouyer et al., 2018).

Under heat stress 29 DE TOR related proteins were identified via a Venn diagram, 20 genes of which are down-regulated and 9 up-regulated (Fig 3.5.6) (Van Leene et al., 2019). Additionally, 125 DE genes were highlighted for the S6K transcription factor target genes under heat stress, with 54 genes down-regulated and 71 genes up-regulated (Fig 3.5.6). This suggests a heat stress related control of S6K target genes. Grouped S6K transcription factor target genes were overlapped in addition to DE *Arabidopsis* heat stress genes (Fig 3.5.7). This generated overlapping target genes from all transcription factors with 56 E2Fa targets genes, 88 RBR1 targets genes and 3 ABA targets overlapping with DE *Arabidopsis* heat stress genes. In addition, 22 of these genes coincided between E2Fa, RBR1 and the *Arabidopsis* HS genes.

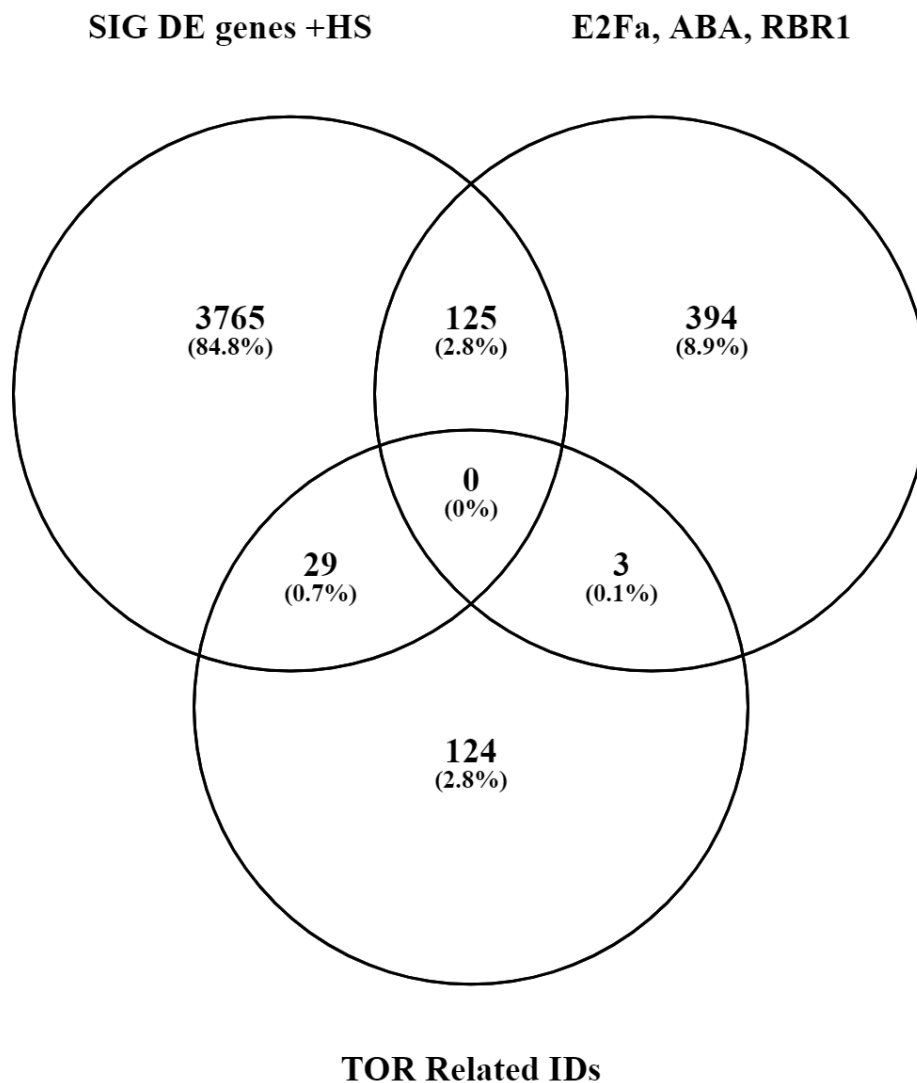


Figure 3.5. 6 Overlap of DE genes under HS in WT Col-0 with TOR interacting proteins and plant S6K TF related IDs

Venn diagram depicts the number and percentage distribution of overlapping significantly DE genes from heat stress RNAseq data. Overlapping with know TOR related protein IDs, a compiled list of transcription factor (TF) target genes, E2Fa top 200, RBR1 stress, ABA-responsive target genes. The top 200 E2Fa-bound genes identified by ChIP, Tandem Chromatin Affinity Purification (TChAP) and Chromatin Affinity Purification (ChAP) (Verkest et al., 2014). ABA Regulated genes from ABI5 activation under drought and salt stress experiments (Skubacz et al., 2016). RBR1 genes upregulated at least once in 32 compiled stress experiments covering all biotic, abiotic stresses, infrared, High energy or gamma radiation Stress experiments, in comparison with RBR1-bound genes were used (Bouyer et al., 2018). TOR interacting proteins were utilised from a pull-down assay by (Van Leene et al., 2019).

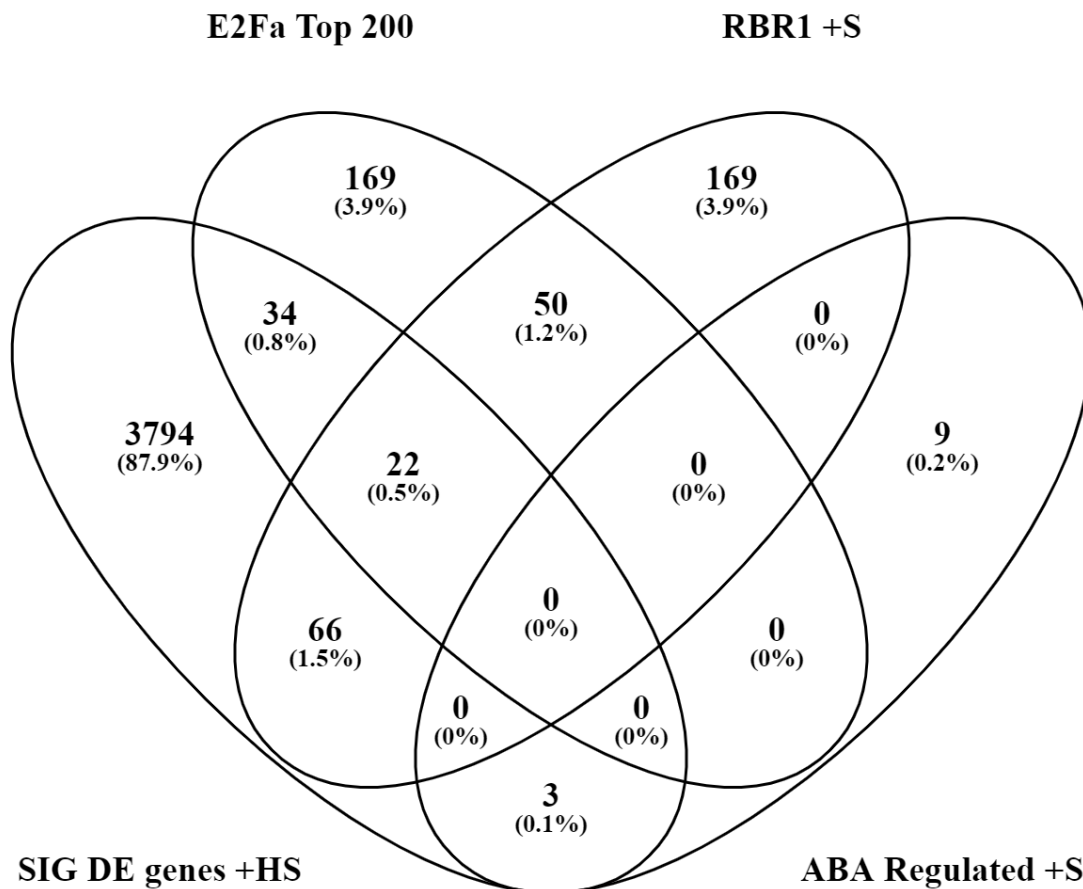


Figure 3.5. 7 Overlapping plant S6K TF target IDs under compiled stresses and DE genes under Heat stress in WT Col-0.

Venn diagram depicts the number and percentage distribution of overlapping significantly DE genes from heat stress RNAseq data with known interacting S6K transcription factors, E2Fa top 200, RBR1 stress, and ABA-responsive target genes. The top 200 E2Fa-bound genes identified by ChIP, Tandem Chromatin Affinity Purification (TChAP) and Chromatin Affinity Purification (ChAP) (Verkest et al., 2014). ABA Regulated +S genes from ABI5 activation under drought and salt stress experiments (Skubacz et al., 2016) RBR1 +S genes upregulated at least once in 32 compiled stress experiments covering all biotic, abiotic stresses, infrared, High energy or gamma radiation Stress experiments, in comparison with RBR1-bound genes were used (Bouyer et al., 2018).

3.5.3 - Overlapping gene data retrieval and GO analysis

The 56 E2Fa targets genes, 88 RBR1 targets genes and 3 ABA targets overlapping with DE *Arabidopsis* genes plus the 22 of these genes coinciding between E2Fa, RBR1 and the *Arabidopsis* HS genes were then retrieved from DE gene list for interpretation. Gene descriptions were obtained by searching the gene Locus IDs in TAIR using the Bulk data retrieval tool (Table 3.5.3.1-3.5.3.5)

(www.Arabidopsisorg/tools). Despite E2F being TOR regulated it was not identified in this study due to the TOR data set being based on using LST8-1 and Raptor1B as bait in the cell culture for the pull-down assay, meaning no E2F family genes were present in the TOR data set. Searching for E2F genes in the DE heat-responsive genes we identified genes that are involved in E2F regulation and activity.

Gene Locus IDs in TAIR using the Bulk data retrieval tool

(www.Arabidopsisorg/tools) was used to search for gene ontologies for overlapping RBR1 stress-induced genes with and DE genes under heat stress. This enabled the determination of any common functions among the downstream target genes by looking at the hypergeometric distribution compared to the *Arabidopsis* background. This was carried out for 88 RBR1 regulated genes being differentially expressed in heat stress and filtered using the Bonferroni adjusted p value at a cut off value of 0.05 (Table 3.5.3.6) (Huang, Sherman and Lempicki, 2008a; Huang, Sherman and Lempicki, 2008b). The RBR1 target genes submitted produced 1 distinct cluster of DNA replication and repair, with a fold enrichment between 9.8 and 235.8 compared to the background (Table 3.5.3.6).

Table 3.5.3. 1 Overlapping TOR related genes with DE heat stress genes

From	To	Gene Name
AT3G49590	F4IXZ6_ARATH	Autophagy-related protein 13(ATG13)
AT1G62740	HSOP2_ARATH	stress-inducible protein(Hop2)
AT3G08730	P93034_ARATH	protein-serine kinase 1(PK1)
AT1G09570	PHYA_ARATH	phytochrome A(PHYA)
AT5G22060	DNAJ2_ARATH	DNAJ homologue 2(J2)
AT2G16570	ASE1_ARATH	GLN phosphoribosyl pyrophosphate amidotransferase 1(ASE1)
AT1G29400	A0A178W1W1_ARATH	MEI2-like protein 5(ML5)
AT4G15410	PUX5_ARATH	serine/threonine protein phosphatase 2A 55 kDa regulatory subunit B prime gamma(PUX5)
AT5G58430	A0A178UIU4_ARATH	exocyst subunit exo70 family protein B1(EXO70B1)
AT3G63130	RAGP1_ARATH	RAN GTPase activating protein 1(RANGAP1)
AT5G56500	A0A178UKH6_ARATH	TCP-1/cpn60 chaperonin family protein(Cpn60beta3)
AT1G05805	BH128_ARATH	basic helix-loop-helix (bHLH) DNA-binding superfamily protein(AT1G05805)
AT3G13470	CPNB2_ARATH	TCP-1/cpn60 chaperonin family protein(Cpn60beta2)
AT1G16030	HSP7E_ARATH	heat shock protein 70B(Hsp70b)
AT3G12580	A0A178VCC0_ARATH	heat shock protein 70(HSP70)
AT3G13860	CH60C_ARATH	heat shock protein 60-3A(HSP60-3A)
AT5G02500	A0A178UL64_ARATH	heat shock cognate protein 70-1(HSC70-1)
AT4G39960	Q940V1_ARATH	Molecular chaperone Hsp40/DnaJ family protein(AT4G39960)
AT2G28000	A0A178VZW6_ARATH	chaperonin-60alpha(CPN60A)
AT1G20630	Q0WUH6_ARATH	catalase 1(CAT1)

Table 3.5.3. 2 Overlapping ABA related genes with DE heat stress genes

From	To	Gene Name
AT2G19450	DGAT1_ARATH	membrane bound O-acyl transferase (MBOAT) family protein(TAG1)
AT5G06860	PGIP1_ARATH	polygalacturonase inhibiting protein 1(PGIP1)
AT5G06870	A0A178UDM1_ARATH	polygalacturonase inhibiting protein 2(PGIP2)

Table 3.5.3. 3 Overlapping top 200 E2F related genes with DE heat stress genes

From	To	Gene Name
AT5G14020	Q0WSL5_ARATH	Endosomal targeting BRO1-like domain-containing protein(AT5G14020)
AT1G80440	FBK30_ARATH	Galactose oxidase/kelch repeat superfamily protein(AT1G80440)
AT3G01600	Q9SS95_ARATH	NAC domain containing protein 44(NAC044)
AT5G41080	F4JWX3_ARATH	PLC-like phosphodiesterases superfamily protein(GDPD2)
AT3G12170	Q9LH49_ARATH	Chaperone DnaJ-domain superfamily protein(AT3G12170)
AT3G46940	DUT_ARATH	DUTP-PYROPHOSPHATASE-LIKE 1(DUT1)
AT3G46620	RDUF1_ARATH	zinc finger (C3HC4-type RING finger) family protein(RDUF1)
AT1G47210	CCA32_ARATH	cyclin-dependent protein kinase 3;2(CYCA3;2)
AT3G52115	A0A178V6G8_ARATH	protein gamma response 1(GR1)
AT3G52115	GR1_ARATH	protein gamma response 1(GR1)
AT3G11520	CCB13_ARATH	CYCLIN B1;3(CYCB1;3)
AT3G48160	E2FE_ARATH	DP-E2F-like 1(DEL1)
AT1G07270	CDC6B_ARATH	Cell division control, Cdc6(AT1G07270)
AT4G01120	O04618_ARATH	G-box binding factor 2(GBF2)
AT5G46740	UBP21_ARATH	ubiquitin-specific protease 21(UBP21)
AT5G24330	A0A178UMD0_ARATH	TRITHORAX-RELATED PROTEIN 6(ATXR6)
AT2G17840	O48832_ARATH	Senescence/dehydration-associated protein-like protein(ERD7)
AT5G63540	RMI1_ARATH	recQ-mediated instability protein (DUF1767)(RMI1)
AT3G59550	SCC13_ARATH	Rad21/Rec8-like family protein(SYN3)
AT2G42260	PYM_ARATH	uv-b-insensitive 4(UVI4)
AT2G42580	TTL3_ARATH	tetratricopetide-repeat thioredoxin-like 3(TTL3)
AT1G26840	ORC6_ARATH	origin recognition complex protein 6(ORC6)
AT5G08020	RFA1B_ARATH	RPA70-kDa subunit B(RPA70B)
AT5G08020	A0A178UED9_ARATH	RPA70-kDa subunit B(RPA70B)
AT3G16740	FBK56_ARATH	F-box and associated interaction domains-containing protein(AT3G16740)
AT5G61000	A0A178UJ91_ARATH	Replication factor-A protein 1-like protein(RPA70D)
AT1G12370	PHR_ARATH	photolyase 1(PHR1)
AT5G24760	ADHL6_ARATH	GroES-like zinc-binding dehydrogenase family protein(AT5G24760)

AT3G56330	Q9LYL0_ARATH	N2,N2-dimethylguanosine tRNA methyltransferase(AT3G56330)
AT5G52950	F4KHP4_ARATH	LIM domain protein(AT5G52950)
AT3G56250	Q9LYL8_ARATH	hypothetical protein(AT3G56250)
AT2G22900	GT7_ARATH	Galactosyl transferase GMA12/MNN10 family protein(AT2G22900)
AT5G43080	CCA31_ARATH	Cyclin A3;1(CYCA3;1)
AT4G28310	Q8LDV4_ARATH	microtubule-associated protein(AT4G28310)
AT1G47230	CCA34_ARATH	CYCLIN A3;4(CYCA3;4)
AT2G02810	UTR1_ARATH	UDP-galactose transporter 1(UTR1)
AT5G56310	A0A178UI86_ARATH	Pentatricopeptide repeat (PPR) superfamily protein(AT5G56310)
AT1G04020	F4I442_ARATH	breast cancer associated RING 1(BARD1)
AT3G48540	Q1PEH3_ARATH	Cytidine/deoxycytidylate deaminase family protein(AT3G48540)
AT3G20490	F4JEP8_ARATH	Rho GTPase-activating protein(AT3G20490)
AT3G48980	Q9SMT6_ARATH	O-glucosyltransferase rumi-like protein (DUF821)(AT3G48980)
AT1G09750	AED3_ARATH	Eukaryotic aspartyl protease family protein(AT1G09750)
AT5G13060	ABAP1_ARATH	ARMADILLO BTB protein 1(ABAP1)
AT2G42110	O23683_ARATH	hypothetical protein(AT2G42110)
AT4G27510	Q5XV71_ARATH	2-isopropylmalate synthase(AT4G27510)
AT4G02110	Y4211_ARATH	transcription coactivator(AT4G02110)
AT5G43530	SM3L3_ARATH	Helicase protein with RING/U-box domain-containing protein(AT5G43530)
AT5G40460	Q29Q81_ARATH	cyclin-dependent kinase inhibitor SMR3-like protein(AT5G40460)
AT3G27640	Q94C55_ARATH	Transducin/WD40 repeat-like superfamily protein(AT3G27640)
AT1G65470	FAS1_ARATH	chromatin assembly factor-1 (FASCIATA1) (FAS1)(FAS1)
AT2G31270	CDT1A_ARATH	CDT1-like protein A(CDT1A)
AT4G22780	ACR7_ARATH	ACT domain repeat 7(ACR7)
AT5G10440	CCD42_ARATH	cyclin d4;2(CYCD4;2)
AT1G75150	F4HXG0_ARATH	DNA ligase-like protein(AT1G75150)
AT4G17680	Q8L7G9_ARATH	SBP (S-ribonuclease binding protein) family protein(AT4G17680)
AT3G14740	Q8L8P1_ARATH	RING/FYVE/PHD zinc finger superfamily protein(AT3G14740)
AT1G20720	F4HUN4_ARATH	RAD3-like DNA-binding helicase protein(AT1G20720)

Table 3.5.3. 4 Overlapping top 200 E2F and RBR1 related genes with DE heat stress genes

From	To	Gene Name
AT4G01120	O04618_ARATH	G-box binding factor 2(GBF2)
AT4G02110	Y4211_ARATH	transcription coactivator(AT4G02110)
AT3G56330	Q9LYL0_ARATH	N2,N2-dimethylguanosine tRNA methyltransferase(AT3G56330)
AT1G12370	PHR_ARATH	photolyase 1(PHR1)
AT5G46740	UBP21_ARATH	ubiquitin-specific protease 21(UBP21)
AT2G17840	O48832_ARATH	Senescence/dehydration-associated protein-like protein(ERD7)
AT3G56250	Q9LYL8_ARATH	hypothetical protein(AT3G56250)
AT3G01600	Q9SS95_ARATH	NAC domain containing protein 44(NAC044)
AT3G59550	SCC13_ARATH	Rad21/Rec8-like family protein(SYN3)
AT5G41080	F4JWX3_ARATH	PLC-like phosphodiesterases superfamily protein(GDPD2)
AT4G28310	Q8LDV4_ARATH	microtubule-associated protein(AT4G28310)
AT3G12170	Q9LH49_ARATH	Chaperone DnaJ-domain superfamily protein(AT3G12170)
AT5G08020	RFA1B_ARATH	RPA70-kDa subunit B(RPA70B)
AT3G46940	DUT_ARATH	DUTP-PYROPHOSPHATASE-LIKE 1(DUT1)
AT5G61000	A0A178UJ91_ARATH	Replication factor-A protein 1-like protein(RPA70D)
AT5G56310	A0A178UI86_ARATH	Pentatricopeptide repeat (PPR) superfamily protein(AT5G56310)
AT1G04020	F4I442_ARATH	breast cancer associated RING 1(BARD1)
AT3G20490	F4JEP8_ARATH	Rho GTPase-activating protein(AT3G20490)
AT3G14740	Q8L8P1_ARATH	RING/FYVE/PHD zinc finger superfamily protein(AT3G14740)
AT5G13060	ABAP1_ARATH	ARMADILLO BTB protein 1(ABAP1)
AT3G11520	CCB13_ARATH	CYCLIN B1;3(CYCB1;3)

Table 3.5.3. 5 Overlapping RBR1 stress related genes with DE heat stress genes

From	To	Gene Name
AT4G00760	APRR8_ARATH	pseudo-response regulator 8(APRR8)
AT4G01010	CNG13_ARATH	cyclic nucleotide-gated channel 13(CNGC13)
AT3G56870	Q5XVA1_ARATH	hypothetical protein(AT3G56870)
AT5G45400	RFA1C_ARATH	Replication factor-A protein 1-like protein(RPA70C)
AT3G55660	ROFG6_ARATH	ROP (rho of plants) guanine nucleotide exchange factor 6(ROPGEF6)
AT4G18290	KAT2_ARATH	potassium channel KAT1-like protein(KAT2)
AT3G52110	Q9SUZ4_ARATH	interferon-activable protein(AT3G52110)
AT1G11380	Q8LFV5_ARATH	PLAC8 family protein(AT1G11380)
AT1G57820	ORTH2_ARATH	Zinc finger (C3HC4-type RING finger) family protein(VIM1)
AT3G01600	Q9SS95_ARATH	NAC domain containing protein 44(NAC044)
AT2G39400	O80627_ARATH	alpha/beta-Hydrolases superfamily protein(AT2G39400)
AT3G02850	A0A178VHK5_ARATH	STELAR K+ outward rectifier(SKOR)
AT2G36010	F4ILT1_ARATH	E2F transcription factor 3(E2F3)
AT5G41080	F4JWX3_ARATH	PLC-like phosphodiesterases superfamily protein(GDPD2)
AT3G12170	Q9LH49_ARATH	Chaperone DnaJ-domain superfamily protein(AT3G12170)
AT3G46940	DUT_ARATH	DUTP-PYROPHOSPHATASE-LIKE 1(DUT1)
AT2G02710	A0A178VU83_ARATH	PAS/LOV protein B(PLPB)
AT4G10960	UGE5_ARATH	UDP-D-glucose/UDP-D-galactose 4-epimerase 5(UGE5)
AT5G12230	MD19A_ARATH	mediator of RNA polymerase II transcription subunit 19a-like protein(MED19A)
AT1G20693	HMGB2_ARATH	high mobility group B2(HMGB2)
AT1G09970	F4I2N7_ARATH	Leucine-rich receptor-like protein kinase family protein(LRR XI-23)
AT4G19130	RFA1E_ARATH	Replication factor-A protein 1-like protein(AT4G19130)
AT3G11520	CCB13_ARATH	CYCLIN B1;3(CYCB1;3)
AT5G22920	Q9FFB6_ARATH	CHY-type/CTCHY-type/RING-type Zinc finger protein(AT5G22920)
AT4G01120	O04618_ARATH	G-box binding factor 2(GBF2)
AT3G05130	Q9MAA6_ARATH	paramyosin-like protein(AT3G05130)
AT5G43630	Q9FIX7_ARATH	zinc knuckle (CCHC-type) family protein(TZP)

AT5G46740	UBP21_ARATH	ubiquitin-specific protease 21(UBP21)
AT2G17840	O48832_ARATH	Senescence/dehydration-associated protein-like protein(ERD7)
AT3G59670	Q56XZ5_ARATH	elongation factor(AT3G59670)
AT3G59550	SCC13_ARATH	Rad21/Rec8-like family protein(SYN3)
AT4G01080	TBL26_ARATH	TRICHOME BIREFRINGENCE-LIKE 26(TBL26)
AT5G08020	RFA1B_ARATH	RPA70-kDa subunit B(RPA70B)
AT1G51340	DTX42_ARATH	MATE efflux family protein(AT1G51340)
AT5G61000	A0A178UJ91_ARATH	Replication factor-A protein 1-like protein(RPA70D)
AT2G38290	AMT2_ARATH	ammonium transporter 2(AMT2)
AT5G04620	A0A178U769_ARATH	biotin F(BIOF)
AT3G10880	Q58FW3_ARATH	tropomyosin(AT3G10880)
AT4G18470	Q9SWA6_ARATH	negative regulator of systemic acquired resistance (SNI1)(SNI1)
AT5G21940	Q9C593_ARATH	hybrid signal transduction histidine kinase M-like protein(AT5G21940)
AT2G25460	Q9SKK3_ARATH	EEIG1/EHBP1 protein amino-terminal domain protein(AT2G25460)
AT4G01550	NAC69_ARATH	NAC domain containing protein 69(NAC069)
AT1G12370	PHR_ARATH	photolyase 1(PHR1)
AT1G61260	F4HTI9_ARATH	cotton fiber (DUF761)(AT1G61260)
AT5G18640	F4JY30_ARATH	alpha/beta-Hydrolases superfamily protein(AT5G18640)
AT3G56330	Q9LYL0_ARATH	N2,N2-dimethylguanosine tRNA methyltransferase(AT3G56330)
AT4G00940	DOF41_ARATH	Dof-type zinc finger DNA-binding family protein(AT4G00940)
AT1G61340	F4HTJ7_ARATH	F-box family protein(FBS1)
AT2G37560	ORC2_ARATH	origin recognition complex second largest subunit 2(ORC2)
AT2G37560	F4IQY6_ARATH	origin recognition complex second largest subunit 2(ORC2)
AT2G39100	Q8VZ73_ARATH	RING/U-box superfamily protein(AT2G39100)
AT2G39220	PLP6_ARATH	PATATIN-like protein 6(PLP6)
AT3G56250	Q9LYL8_ARATH	hypothetical protein(AT3G56250)
AT5G21170	Q29Q48_ARATH	5'-AMP-activated protein kinase beta-2 subunit protein(AKINBETA1)
AT4G07410	Q8RXU6_ARATH	Transducin family protein / WD-40 repeat family protein(PCN)
AT2G38250	A0A178VPR5_ARATH	Homeodomain-like superfamily protein(AT2G38250)
AT5G14960	E2FD_ARATH	DP-E2F-like 2(DEL2)
AT1G09080	A0A178WHW4_ARATH	Heat shock protein 70 (Hsp 70) family protein(BIP3)

AT4G28310	Q8LDV4_ARATH	microtubule-associated protein(AT4G28310)
AT2G17230	EXOL5_ARATH	EXORDIUM like 5(EXL5)
AT4G36010	O65638_ARATH	Pathogenesis-related thaumatin superfamily protein(AT4G36010)
AT3G12270	ANM3_ARATH	protein arginine methyltransferase 3(PRMT3)
AT5G58770	B5X0P4_ARATH	Undecaprenyl pyrophosphate synthetase family protein(cPT4)
AT2G43160	EPN2_ARATH	ENTH/VHS family protein(AT2G43160)
AT5G56310	A0A178UI86_ARATH	Pentatricopeptide repeat (PPR) superfamily protein(AT5G56310)
AT1G77760	A0A178WBR8_ARATH	nitrate reductase 1(NIA1)
AT2G22500	PUMP5_ARATH	uncoupling protein 5(UCP5)
AT1G04020	F4I442_ARATH	breast cancer associated RING 1(BARD1)
AT3G20490	F4JEP8_ARATH	Rho GTPase-activating protein(AT3G20490)
AT5G13060	ABAP1_ARATH	ARMADILLO BTB protein 1(ABAP1)
AT5G48820	A0A178UGC0_ARATH	inhibitor/interactor with cyclin-dependent kinase(ICK6)
AT5G48820	KRP3_ARATH	inhibitor/interactor with cyclin-dependent kinase(ICK6)
AT4G02110	Y4211_ARATH	transcription coactivator(AT4G02110)
AT3G27640	Q94C55_ARATH	Transducin/WD40 repeat-like superfamily protein(AT3G27640)
AT5G19920	Q8GX62_ARATH	Transducin/WD40 repeat-like superfamily protein(AT5G19920)
AT2G39110	Q0WSF6_ARATH	Protein kinase superfamily protein(AT2G39110)
AT2G38340	DRE2E_ARATH	Integrase-type DNA-binding superfamily protein(DREB19)
AT5G46080	Q9FNL4_ARATH	Protein kinase superfamily protein(AT5G46080)
AT5G66230	F4JZ53_ARATH	Chalcone-flavanone isomerase family protein(AT5G66230)
AT2G36880	A0A178VXF8_ARATH	methionine adenosyltransferase 3(MAT3)
AT1G68190	COLX_ARATH	B-box zinc finger family protein(BBX27)
AT1G52530	Q709F6_ARATH	Hus1-like protein(AT1G52530)
AT2G01610	Q9ZNU5_ARATH	Plant invertase/pectin methylesterase inhibitor superfamily protein(AT2G01610)
AT2G39360	Y2393_ARATH	Protein kinase superfamily protein(AT2G39360)
AT5G02220	Q1JPP8_ARATH	cyclin-dependent kinase inhibitor(AT5G02220)
AT3G14740	Q8L8P1_ARATH	RING/FYVE/PHD zinc finger superfamily protein(AT3G14740)

AT2G44500	F4IU48_ARATH	O-fucosyltransferase family protein(AT2G44500)
AT5G22930	F4KBD8_ARATH	enabled-like protein (DUF1635)(AT5G22930)
AT4G17760	Q8L7G8_ARATH	PCNA domain-containing protein(AT4G17760)
AT1G79150	F4IDJ0_ARATH	binding protein(AT1G79150)

Table 3.5.3. 6 GO analysis of up-regulated overlapping RBR1 stress related genes with DE heat stress genes

Cluster 1		
Term	Fold Enrichment	Bonferroni
IPR004591:Replication factor-a protein 1 Rpa1	235.7866667	5.73E-05
IPR007199:Replication factor-A protein 1, N-terminal	235.7866667	5.73E-05
IPR013955:Replication factor A, C-terminal	147.3666667	3.19E-04
IPR004365:Nucleic acid binding, OB-fold, tRNA/helicase-type	73.68333333	0.003122477
GO:0006281~DNA repair	9.816024864	0.011773774
DNA replication	21.79146141	0.009160183
DNA repair	13.07487685	0.010743977
DNA damage	12.36812675	0.013933416
GO:0006260~DNA replication	16.00259516	0.040997816
ath03430:Mismatch repair	28.5188537	0.005655678
ath03030:DNA replication	22.24470588	0.01182159
ath03440:Homologous recombination	19.86134454	0.016475852
ath03420:Nucleotide excision repair	16.11935209	0.030114554

Chapter 4 - Discussion

The S6Ks are a group of serine/threonine kinase in the AGC family active under the TOR pathway, these regulate and control many other cellular processes. With mutants resulting in embryonic lethality. The limited number of identified interacting proteins leaves this pathway relatively uncharacterised.

This thesis has shown that AtS6K isoforms have some overlapping targets but also some alternate ones (Mockler et al., 2007). Considering the number of limited influencing factors and structures this project aims to fill the gaps in the knowledge regarding interacting proteins and transcription factors and RNA outputs. The use of recombinant DNA technology enabled AtS6K1 genes to be amplified and inserted into pGEX (GST) and pET-21a+ (C terminal HIS) expression vectors, this was successful for both vectors all constructs full length (Figure 3.1.4 and 3.1.7), kinase long (Figure 3.1.5 and 3.1.8) and Kinase domain (Figure 3.1.6 and 3.1.9).

4.1 - Protein expression

The novel purification of GST tagged AtS6K1 constructs was proven to be ineffective in test expression or for production in large amounts. The presence of the GST tag itself being expressed alone has been previously documented with there being a higher affinity for the GST, resulting in GST production without attached protein. Expression and purification were attempted utilising auto-induction media and visualising steps in which the protein may have been lost, however giving the same result. Originally a promising band was seen at 80 KDa however it was present in all constructs, later being identified as the chaperoning protein GroEL. Small amounts

of protein were visualised in the expected regions but were not significant enough for further purification leading to a change in approach.

As a result, an alternate path was chosen cloning and expressing using HIS tagged construct, this would circumvent the high affinity issue with the tag region being located at the end of the protein. After successful recombinant techniques and sequencing, test expression was attempted. This gave no expression of the protein being seen with little cellular protein also being produced. Alternative cell lines were tested to determine if the BL21 cells were defective but also gave the same result. This research was heavily impacted by unforeseen circumstances (Global pandemic).

4.2 - Plant work

Previous work on the cellular localisation of the AtS6K isoforms have been deduced but the effects of stress on their movements are still very sparse. As a result, fluorescent microscopy was enlisted in combination with golden gate cloning due to it's ability to combine the many elements needed for the AtS6K1 constructs.

Including the varying length promoters to ensure the entire promoter would be included and fluorescent tags for spatial visualisation. This would allow the impact of different stresses to be tied to S6K cellular location under fluorescent microscopy.

The unsuccessful cloning of these constructs within the reduced unforeseen timeframe available (Global pandemic) prevented further progress in this area.

4.3 - RNA sequencing

The ability of stress to influence the expression of AtS6k isoforms has been documented but the downstream effect of the transcription factors targets is limited. One example is the TF AtRBR1 that binds with AtS6K1 under nutrient limiting conditions repressing cell proliferation (Henriques et al., 2010). As such RBR1 genes upregulated at least once in 32 compiled stress experiments covering all biotic, abiotic stresses, infrared, High energy or gamma radiation Stress experiments, in comparison with RBR1-bound genes were used (Bouyer et al., 2018).

RBR1 has also been shown to interact and inhibit transcription factor E2Fs, with co-immunoprecipitation experiments suggesting an association with the AtRBR-E2Fs complex (Berckmans and De Veylder, 2009). This is reflected from the overlapping genes highlighted in (Fig 3.5.7) with 22 common genes between the 56 E2F and 88 RBR1 genes submitted. RBR-E2F complexes have been identified to form in both animals and plants, controlling S-phase entry where RBR1 binds and inhibits E2F transcription factors thereby preventing the expression of S-phase genes (Berckmans and De Veylder, 2009).

One interesting role of E2Fa is its ability to control the expression of RNR (RiboNucleotide Reductase), an enzyme involved in deoxyribonucleotide biosynthesis that is strongly activated by DNA damage (Roa et al., 2009). This was the most enriched cluster under heat stress (Table 3.5.3.5). A study by Horvath et al. (2017) showed that silencing of RBR1 triggers DNA damage and cell death in root tips even in the absence of exogenous stress, repressing the expression of several DDR (DNA damage repair) genes in an E2Fa-dependent manner (Biedermann et al.,

2017; Horvath et al., 2017). It is still unclear whether this pathway is triggered by heat stress but the generation of Reactive Oxygen Species (ROS) when plants are exposed to excess heat reduces the plant's capacity to utilise light in its photosystems, which can induce DDR (Noctor and Foyer, 2016).

Significantly differentially expressed genes that overlap with the RNAseq heat stress data or additional transcription factors were selected for highlighting key genes and potentially under multiple TFs (Fig 3.5.7). AtS6K1 was visualised to have significant temporal variation under HS contradicting earlier studies, however confirming its ability to be influenced under heat stresses in the TOR related protein data set (Fig 3.5.5). A large proportion of genes first identified were chaperone proteins that are expected to change, due to their role in preventing the misfolding of proteins under heat stress conditions.

The upregulation of RBR1 genes is expected under heat stress with RBR1 seen in the literature, associating with genes that are highly enriched in DNA repair from actively dividing cells. Also having involved in the negative regulation of the cell cycle, repression of euchromatic genes and endosperm development (Bouyer et al., 2018).

The limited DE ABA genes seen under heat stress provides a weak ABA response when overlaid with heat stress data, however a limited number of input genes due to few known targets reduces evidence to support. With no significant DE of AtS6K2 seen would suggest an alternate means of activation if clarified (Fig 3.5.5) This data suggest that ABA may not be important in regulating TOR activity and downstream signalling pathways.

The atypical E2F transcription factor DEL1 that modulates growth–defence was significantly up-regulated (Table 3.5.3.3) (Nakagami et al., 2020). DEL2 was also significantly up-regulated having roles in increasing the expression of E2FA, E2FB and E2FE/DEL1 when overexpressed (Table 3.5.3.5). Concurrently, DEL2 inactivation leads to the up regulation of genes encoding repressors of cell division (Sozzani et al., 2009). E2F3 a member of the E2F transcription factors, key components of the cyclin D/retinoblastoma/E2F pathway and cell cycle genes were significantly up-regulated (Table 3.5.3.5) (www.arabidopsis.org). The target of the E2F/DF family of transcription factors Origin Recognition Complex subunit 6 (ORC6) (Table 3.5.3.3) and subunit 2 (ORC2) (Table 3.5.3.5) were both up-regulated (www.arabidopsis.org). And finally, SNI1 a protein that interacts with and inhibits E2F transcription factors was also upregulated (Table 3.5.3.5) (www.arabidopsis.org).

4.4 - Conclusion and Future direction

The classical cloning approach taken for the tagged AtS6K1 constructs was proven to be greatly successful into both pGEX-6p-1 (N-terminal GST) and Pet-21a (+) (C-terminal His) vectors. Continuing this work into the expression and purification of AtS6K1 construct would be of great interest, for the determination of both isoforms 3D structure is yet to be solved. Alternatively, other tags could be utilised such as an Myc tag that binds to cMyc Monoclonal antibody. This can also lower the metabolic load increasing protein expression that was minimal in this research. Additionally, purified protein would enable the identification of isoform specific transcription factor interactions via binding studies, elucidating the physical networks with these kinases.

The generation of complex constructs via golden gate cloning showed great promise, achieving very fast and efficient results. This would enable both transient transfection and stable transfection integrating the constructs via ago bacterium. More time allocated to this area could finally help the determination of cellular localisation and expression of AtS6K1 under environmental stress.

The understanding of ribosomal phosphorylation first developed after being documented in 1970 (Loeb and Blat, 1970). Phosphorylation by S6Ks was first noted only 20 years ago in plants (Zhang et al., 1994a; Zhang et al., 1994b) and 30 years ago in humans (Krieg et al., 1988) with the understanding of ribosome phosphorylation only. Since the discovery of plant S6Ks, the general focus on these kinases has grown rapidly, driven by the correlation between these kinases and diseases in humans (Tavares et al., 2015). Very little light has been shed on the biological roles of the S6K family in plants, but strong evidence suggests that S6Ks regulate responses to stresses and developmental cues (Turck et al., 2004; Mahfouz et al., 2006; Rajamaki et al., 2017). The investigation at the transcription levels of plant S6Ks under abiotic stresses is still very sparse, with current work only highlighting the effects of cold and salinity stresses (Mizoguchi et al., 1995). Response to other stresses, such as drought, hypoxia, UV-B, genotoxic, oxidative, and osmotic stress has been shown in publicly available transcriptomic repositories, suggesting roles in response to other stresses (Winter et al., 2007; Hruz et al., 2008). Furthermore, it has still not yet been determined if this variation in S6Ks transcript level correlates to greater production of protein or activity. The complex and diverse roles of the S6K isoforms in plants adapting to external environments warrants further investigation into these proteins.

References

- Ahn, C., Han, J., Lee, H., Lee, S. and Pai, H., 2011. The PP2A Regulatory Subunit Tap46, a Component of the TOR Signaling Pathway, Modulates Growth and Metabolism in Plants. *The Plant Cell*, 23(1), pp.185-209.
- Alcázar, R., Marco, F., Cuevas, J., Patron, M., Ferrando, A., Carrasco, P., Tiburcio, A. and Altabella, T., 2006. Involvement of polyamines in plant response to abiotic stress. *Biotechnology Letters*, 28(23), pp.1867-1876.
- Bechtold, U. and Field, B., 2018a. Molecular mechanisms controlling plant growth during abiotic stress. *Journal of Experimental Botany*, 69(11), pp.2753-2758.
- Bechtold, U., Ferguson, J. and Mullineaux, P., 2018b. To defend or to grow: lessons from *Arabidopsis* C24. *Journal of Experimental Botany*, 69(11), pp.2809-2821.
- Beltran-Pena, E., Aguilar, R., Ortiz-Lopez, A., Dinkova, T. and de Jimenez, E., 2002. Auxin stimulates S6 ribosomal protein phosphorylation in maize thereby affecting protein synthesis regulation. *Physiologia Plantarum*, 115(2), pp.291-297.
- Berckmans, B. and De Veylder, L., 2009. Transcriptional control of the cell cycle. *Current Opinion in Plant Biology*, 12(5), pp.599-605.
- Biedermann, S., Harashima, H., Chen, P., Heese, M., Bouyer, D., Sofroni, K. and Schnittger, A., 2017. The retinoblastoma homolog RBR 1 mediates localization of the repair protein RAD 51 to DNA lesions in *Arabidopsis*. *The EMBO Journal*, 36(9), pp.1279-1297.
- Biondi, R., Cheung, P., Casamayor, A., Deak, M., Currie, R. and Alessi, D., 2000. Identification of a pocket in the PDK1 kinase domain that interacts with PIF and the C-terminal residues of PKA. *The EMBO Journal*, 19(5), pp.979-988.
- Bögge, L., 2003. Growth signalling pathways in *Arabidopsis* and the AGC protein kinases. *Trends in Plant Science*, 8(9), pp.424-431.
- Bouyer, D., Heese, M., Chen, P., Harashima, H., Roudier, F., Grüttner, C. and Schnittger, A., 2018. Genome-wide identification of retinoblastoma related 1 binding sites in *Arabidopsis* reveals novel dna damage regulators. *PLOS Genetics*, 14(11), p.e1007797.
- Bray, N., Pimentel, H., Melsted, P. and Pachter, L., 2016. Near-optimal probabilistic RNA-seq quantification. *Nature Biotechnology*, 34(5), pp.525-527.
- Calixto, C., Guo, W., James, A., Tzioutziou, N., Entizne, J., Panter, P., Knight, H., Nimmo, H., Zhang, R. and Brown, J., 2018. Rapid and Dynamic Alternative Splicing Impacts the *Arabidopsis* Cold Response Transcriptome. *The Plant Cell*, 30(7), pp.1424-1444.
- Calixto, C., Guo, W., James, A., Tzioutziou, N., Entizne, J., Panter, P., Knight, H., Nimmo, H., Zhang, R. and Brown, J., 2018. Rapid and Dynamic Alternative Splicing Impacts the *Arabidopsis* Cold Response Transcriptome. *The Plant Cell*, 30(7), pp.1424-1444.

- Chang, I., Szick-Miranda, K., Pan, S. and Bailey-Serres, J., 2005. Proteomic Characterization of Evolutionarily Conserved and Variable Proteins of Arabidopsis Cytosolic Ribosomes. *Plant Physiology*, 137(3), pp.848-862.
- Creff, A., Sormani, R. and Desnos, T., 2010. The two Arabidopsis RPS6 genes, encoding for cytoplasmic ribosomal proteins S6, are functionally equivalent. *Plant Molecular Biology*, 73(4-5), pp.533-546.
- Deprost, D., Yao, L., Sormani, R., Moreau, M., Leterreux, G., Nicolai, M., Bedu, M., Robaglia, C. and Meyer, C., 2007. The Arabidopsis TOR kinase links plant growth, yield, stress resistance and mRNA translation. *EMBO reports*, 8(9), pp.864-870.
- Dobrenel, T., Caldana, C., Hanson, J., Robaglia, C., Vincentz, M., Veit, B. and Meyer, C., 2016. TOR Signaling and Nutrient Sensing. *Annual Review of Plant Biology*, 67(1), pp.261-285.
- Endicott, J., Noble, M. and Johnson, L., 2012. The Structural Basis for Control of Eukaryotic Protein Kinases. *Annual Review of Biochemistry*, 81(1), pp.587-613.
- Enganti, R., Cho, S., Toperzer, J., Urquidi-Camacho, R., Cakir, O., Ray, A., Abraham, P., Hettich, R. and von Arnim, A., 2018. Phosphorylation of Ribosomal Protein RPS6 Integrates Light Signals and Circadian Clock Signals. *Frontiers in Plant Science*, 8.
- Engelman, J., Luo, J. and Cantley, L., 2006. The evolution of phosphatidylinositol 3-kinases as regulators of growth and metabolism. *Nature Reviews Genetics*, 7(8), pp.606-619.
- Feldman, M., Apsel, B., Uotila, A., Loewith, R., Knight, Z., Ruggero, D. and Shokat, K., 2009. Active-Site Inhibitors of mTOR Target Rapamycin-Resistant Outputs of mTORC1 and mTORC2. *PLoS Biology*, 7(2), p.e1000038.
- García Flores, C., Aguilar, R., Reyes De La Cruz, H., Albores, M. and Sánchez de Jiménez, E., 2001. A maize insulin-like growth factor signals to a transduction pathway that regulates protein synthesis in maize. *Biochemical Journal*, 358(1), p.95.
- Gasteiger, E., 2003. ExPASy: the proteomics server for in-depth protein knowledge and analysis. *Nucleic Acids Research*, 31(13), pp.3784-3788.
- Guo, W., Tzioutziou, N., Stephen, G., Milne, I., Calixto, C., Waugh, R., Brown, J. and Zhang, R., 2020. 3D RNA-seq: a powerful and flexible tool for rapid and accurate differential expression and alternative splicing analysis of RNA-seq data for biologists. *RNA Biology*, pp.1-14.
- Henriques, R., Magyar, Z., Monardes, A., Khan, S., Zalejski, C., Orellana, J., Szabados, L., de la Torre, C., Koncz, C. and Bögre, L., 2010. Arabidopsis S6 kinase mutants display chromosome instability and altered RBR1–E2F pathway activity. *The EMBO Journal*, 29(17), pp.2979-2993.
- Horvath, B., Kourova, H., Nagy, S., Nemeth, E., Magyar, Z., Papdi, C., Ahmad, Z., Sanchez-Perez, G., Perilli, S., Blilou, I., Pettkó-Szandtner, A., Darula, Z., Meszaros, T., Binarova, P., Bogre, L. and Scheres, B., 2017. Arabidopsis retinoblastoma

related directly regulates DNA damage responses through functions beyond cell cycle control. *The EMBO Journal*, 36(9), pp.1261-1278.

Huang, D., Sherman, B. and Lempicki, R., 2008a. Systematic and integrative analysis of large gene lists using DAVID bioinformatics resources. *Nature Protocols*, 4(1), pp.44-57.

Huang, D., Sherman, B. and Lempicki, R., 2008b. Bioinformatics enrichment tools: paths toward the comprehensive functional analysis of large gene lists. *Nucleic Acids Research*, 37(1), pp.1-13.

Huse, M. and Kuriyan, J., 2002. The Conformational Plasticity of Protein Kinases. *Cell*, 109(3), pp.275-282.

Jeno, P., Ballou, L., Novak-Hofer, I. and Thomas, G., 1988. Identification and characterization of a mitogen-activated S6 kinase. *Proceedings of the National Academy of Sciences*, 85(2), pp.406-410.

Kannan, N., Haste, N., Taylor, S. and Neuwald, A., 2007. The hallmark of AGC kinase functional divergence is its C-terminal tail, a cis-acting regulatory module. *Proceedings of the National Academy of Sciences*, 104(4), pp.1272-1277.

Khandal, D., Samol, I., Buhr, F., Pollmann, S., Schmidt, H., Clemens, S., Reinbothe, S. and Reinbothe, C., 2009. Singlet oxygen-dependent translational control in the *tigrina-d.12* mutant of barley. *Proceedings of the National Academy of Sciences*, 106(31), pp.13112-13117.

Kilian, J., Whitehead, D., Horak, J., Wanke, D., Weinl, S., Batistic, O., D'Angelo, C., Bornberg-Bauer, E., Kudla, J. and Harter, K., 2007. The AtGenExpress global stress expression data set: protocols, evaluation and model data analysis of UV-B light, drought and cold stress responses. *The Plant Journal*, 50(2), pp.347-363.

Kim, D., Paggi, J., Park, C., Bennett, C. and Salzberg, S., 2019. Graph-based genome alignment and genotyping with HISAT2 and HISAT-genotype. *Nature Biotechnology*, 37(8), pp.907-915.

Kim, T., Kim, B., Yahalom, A., Chamovitz, D. and von Arnim, A., 2004. Translational Regulation via 5' mRNA Leader Sequences Revealed by Mutational Analysis of the *Arabidopsis* Translation Initiation Factor Subunit eIF3h. *The Plant Cell*, 16(12), pp.3341-3356.

Krieg, J., Hofsteenge, J., and Thomas, G., 1988. Identification of the 40 S ribosomal protein S6 phosphorylation sites induced by cycloheximide. *J. Biol. Chem.* 263 (23), 11473–11477. doi:10.1016/s0021-9258(18)37981-x.

Lai, K., Leong, W., Chau, J., Jia, D., Zeng, L., Liu, H., He, L., Hao, A., Zhang, H., Meek, D., Velagapudi, C., Habib, S. and Li, B., 2010. S6K1 is a multifaceted regulator of Mdm2 that connects nutrient status and DNA damage response. *The EMBO Journal*, 29(17), pp.2994-3006.

Larkin, M., Blackshields, G., Brown, N., Chenna, R., McGettigan, P., McWilliam, H., Valentin, F., Wallace, I., Wilm, A., Lopez, R., Thompson, J., Gibson, T. and Higgins, D., 2007. Clustal W and Clustal X version 2.0. *Bioinformatics*, 23(21), pp.2947-2948.

- Lee, D., Park, S., Ahn, C. and Pai, H., 2017. MRF Family Genes Are Involved in Translation Control, Especially under Energy-Deficient Conditions, and Their Expression and Functions Are Modulated by the TOR Signaling Pathway. *The Plant Cell*, 29(11), pp.2895-2920.
- Levy, S., Avni, D., Hariharan, N., Perry, R. and Meyuhas, O., 1991. Oligopyrimidine tract at the 5' end of mammalian ribosomal protein mRNAs is required for their translational control. *Proceedings of the National Academy of Sciences*, 88(8), pp.3319-3323.
- Li, F. and Vierstra, R., 2012. Regulator and substrate. *Autophagy*, 8(6), pp.982-984.
- Li, L., Zhu, T., Song, Y., Feng, L., Farag, E. and Ren, M., 2021. ABSCISIC ACID INSENSITIVE5 Interacts With RIBOSOMAL S6 KINASE2 to Mediate ABA Responses During Seedling Growth in Arabidopsis. *Frontiers in Plant Science*, 11.
- Loeb, J. E., and Blat, C., 1970. Phosphorylation of some rat liver ribosomal proteins and its activation by cyclic AMP. *FEBS Lett.* 10 (2), 105–108. doi:10. 1016/0014-5793(70)80427-6
- Maegawa, K., Takii, R., Ushimaru, T. and Kozaki, A., 2015. Evolutionary conservation of TORC1 components, TOR, Raptor, and LST8, between rice and yeast. *Molecular Genetics and Genomics*, 290(5), pp.2019-2030.
- Magnuson, B., Ekim, B. and Fingar, D., 2011. Regulation and function of ribosomal protein S6 kinase (S6K) within mTOR signalling networks. *Biochemical Journal*, 441(1), pp.1-21.
- Mahfouz, M., Kim, S., Delauney, A. and Verma, D., 2005. Arabidopsis TARGET OF RAPAMYCIN Interacts with RAPTOR, Which Regulates the Activity of S6 Kinase in Response to Osmotic Stress Signals. *The Plant Cell*, 18(2), pp.477-490.
- Margalha, L., Confraria, A. and Baena-González, E., 2019. SnRK1 and TOR: modulating growth–defense trade-offs in plant stress responses. *Journal of Experimental Botany*, 70(8), pp.2261-2274.
- Mockler, T., Michael, T., Priest, H., Shen, R., Sullivan, C., Givan, S., McEntee, C., Kay, S. and Chory, J., 2007. The Diurnal Project: Diurnal and Circadian Expression Profiling, Model-based Pattern Matching, and Promoter Analysis. *Cold Spring Harbor Symposia on Quantitative Biology*, 72(1), pp.353-363.
- Montagne, J., 1999. Drosophila S6 Kinase: A Regulator of Cell Size. *Science*, 285(5436), pp.2126-2129.
- Nakagami, S., Saeki, K., Toda, K., Ishida, T. and Sawa, S., 2020. The atypical E2F transcription factor DEL1 modulates growth–defense tradeoffs of host plants during root-knot nematode infection. *Scientific Reports*, 10(1).
- Noctor, G. and Foyer, C., 2016. Intracellular Redox Compartmentation and ROS-Related Communication in Regulation and Signaling. *Plant Physiology*, 171(3), pp.1581-1592.

Nolen, B., Taylor, S. and Ghosh, G., 2004. Regulation of Protein Kinases. *Molecular Cell*, 15(5), pp.661-675.

Piques, M., Schulze, W., Höhne, M., Usadel, B., Gibon, Y., Rohwer, J. and Stitt, M., 2009. Ribosome and transcript copy numbers, polysome occupancy and enzyme dynamics in *Arabidopsis*. *Molecular Systems Biology*, 5(1), p.314.

Rademacher, E. and Offringa, R., 2012. Evolutionary Adaptations of Plant AGC Kinases: From Light Signaling to Cell Polarity Regulation. *Frontiers in Plant Science*, 3.

Ren, M., Venglat, P., Qiu, S., Feng, L., Cao, Y., Wang, E., Xiang, D., Wang, J., Alexander, D., Chalivendra, S., Logan, D., Mattoo, A., Selvaraj, G. and Datla, R., 2012. Target of Rapamycin Signaling Regulates Metabolism, Growth, and Life Span in *Arabidopsis*. *The Plant Cell*, 24(12), pp.4850-4874.

Rexin, D., Meyer, C., Robaglia, C. and Veit, B., 2015. TOR signalling in plants. *Biochemical Journal*, 470(1), pp.1-14.

Roa, H., Lang, J., Culligan, K., Keller, M., Holec, S., Cognat, V., Montané, M., Houlné, G. and Chabouté, M., 2009. Ribonucleotide Reductase Regulation in Response to Genotoxic Stress in *Arabidopsis*. *Plant Physiology*, 151(1), pp.461-471.

Robaglia, C., Thomas, M. and Meyer, C., 2012. Sensing nutrient and energy status by SnRK1 and TOR kinases. *Current Opinion in Plant Biology*, 15(3), pp.301-307.

Rosado, A., Li, R., van de Ven, W., Hsu, E. and Raikhel, N., 2012. *Arabidopsis* ribosomal proteins control developmental programs through translational regulation of auxin response factors. *Proceedings of the National Academy of Sciences*, 109(48), pp.19537-19544.

Rossi, R., Pester, J., McDowell, M., Soza, S., Montecucco, A. and Lee-Fruman, K., 2007. Identification of S6K2 as a centrosome-located kinase. *FEBS Letters*, 581(21), pp.4058-4064.

Roux, P., Shahbazian, D., Vu, H., Holz, M., Cohen, M., Taunton, J., Sonenberg, N. and Blenis, J., 2007. RAS/ERK Signaling Promotes Site-specific Ribosomal Protein S6 Phosphorylation via RSK and Stimulates Cap-dependent Translation. *Journal of Biological Chemistry*, 282(19), pp.14056-14064.

Sánchez de Jiménez, E., Beltrán-Peña, E. and Ortíz-López, A., 1999. Insulin-stimulated ribosomal protein synthesis in maize embryonic axes during germination. *Physiologia Plantarum*, 105(1), pp.148-154.

Sarbassov, D. (2005). Phosphorylation and Regulation of Akt/PKB by the Rictor-mTOR Complex. *Science*, 307(5712), pp.1098-1101.

Scharf, K. and Nover, L., 1982. Heat-shock-induced alterations of ribosomal protein phosphorylation in plant cell cultures. *Cell*, 30(2), pp.427-437.

Schepetilnikov, M., Dimitrova, M., Mancera-Martínez, E., Geldreich, A., Keller, M. and Ryabova, L., 2013. TOR and S6K1 promote translation reinitiation of uORF-

containing mRNAs via phosphorylation of eIF3h. *The EMBO Journal*, 32(8), pp.1087-1102.

Schepetilnikov, M., Kobayashi, K., Geldreich, A., Caranta, C., Robaglia, C., Keller, M. and Ryabova, L., 2011. Viral factor TAV recruits TOR/S6K1 signalling to activate reinitiation after long ORF translation. *The EMBO Journal*, 30(7), pp.1343-1356.

Sengupta, S., Peterson, T. and Sabatini, D., 2010. Regulation of the mTOR Complex 1 Pathway by Nutrients, Growth Factors, and Stress. *Molecular Cell*, 40(2), pp.310-322.

Shin, Y., Kim, S., Du, H., Choi, S., Verma, D. and Cheon, C., 2012. Possible dual regulatory circuits involving AtS6K1 in the regulation of plant cell cycle and growth. *Molecules and Cells*, 33(5), pp.487-496.

Skubacz, A., Daszkowska-Golec, A. and Szarejko, I., 2016. The Role and Regulation of ABI5 (ABA-Insensitive 5) in Plant Development, Abiotic Stress Responses and Phytohormone Crosstalk. *Frontiers in Plant Science*, 7.

Son, O., Kim, S., Hur, Y. and Cheon, C., 2017. Molecular details of the Raptor-binding motif on Arabidopsis S6 kinase. *Biochemical and Biophysical Research Communications*, 486(1), pp.137-142.

Sozzani, R., Maggio, C., Giordo, R., Umana, E., Ascencio-Ibañez, J., Hanley-Bowdoin, L., Bergounioux, C., Cella, R. and Albani, D., 2009. The E2FD/DEL2 factor is a component of a regulatory network controlling cell proliferation and development in Arabidopsis. *Plant Molecular Biology*, 72(4-5), pp.381-395.

Sun, L., Yu, Y., Hu, W., Min, Q., Kang, H., Li, Y., Hong, Y., Wang, X. and Hong, Y., 2016. Ribosomal protein S6 kinase1 coordinates with TOR-Raptor2 to regulate thylakoid membrane biosynthesis in rice. *Biochimica et Biophysica Acta (BBA) - Molecular and Cell Biology of Lipids*, 1861(7), pp.639-649.

Tavares, M. R., Pavan, I. C. B., Amaral, C. L., Meneguello, L., Luchessi, A. D., & Simabuco, F. M., 2015. The S6K protein family in health and disease. *Life Sciences*, 131, 1–10. doi:10.1016/j.lfs.2015.03.001.

Thiébeauld, O., Schepetilnikov, M., Park, H., Geldreich, A., Kobayashi, K., Keller, M., Hohn, T. and Ryabova, L., 2009. A new plant protein interacts with eIF3 and 60S to enhance virus-activated translation re-initiation. *The EMBO Journal*, 28(20), pp.3171-3184.

Tm Calculator last used January, 2020,
<http://www6.appliedbiosystems.com/support/techttools/calc/>

Turck, F., Kozma, S., Thomas, G. and Nagy, F., 1998. A Heat-Sensitive Arabidopsis thaliana Kinase Substitutes for Human p70s6k Function In Vivo. *Molecular and Cellular Biology*, 18(4), pp.2038-2044.

Turck, F., Zilbermann, F., Kozma, S., Thomas, G. and Nagy, F., 2004. Phytohormones Participate in an S6 Kinase Signal Transduction Pathway in Arabidopsis. *Plant Physiology*, 134(4), pp.1527-1535.

Turkina, M., Klang Årstrand, H. and Vener, A., 2011. Differential Phosphorylation of Ribosomal Proteins in *Arabidopsis thaliana* Plants during Day and Night. *PLoS ONE*, 6(12), p.e29307.

van den Heuvel, S. and Dyson, N., 2008. Conserved functions of the pRB and E2F families. *Nature Reviews Molecular Cell Biology*, 9(9), pp.713-724.

Van Leene, J., Han, C., Gadeyne, A., Eeckhout, D., Matthijs, C., Cannoot, B., De Winne, N., Persiau, G., Van De Slijke, E., Van de Cotte, B., Stes, E., Van Bel, M., Storme, V., Impens, F., Gevaert, K., Vandepoele, K., De Smet, I. and De Jaeger, G., 2019. Capturing the phosphorylation and protein interaction landscape of the plant TOR kinase. *Nature Plants*, 5(3), pp.316-327.

Verkest, A., Abeel, T., Heyndrickx, K., Van Leene, J., Lanz, C., Van De Slijke, E., De Winne, N., Eeckhout, D., Persiau, G., Van Breusegem, F., Inzé, D., Vandepoele, K. and De Jaeger, G., 2014. A Generic Tool for Transcription Factor Target Gene Discovery in *Arabidopsis* Cell Suspension Cultures Based on Tandem Chromatin Affinity Purification. *Plant Physiology*, 164(3), pp.1122-1133.

Vézina, C., Kudelski, A. and Sehgal, S., 1975. Rapamycin (AY-22,989), a new antifungal antibiotic. I. Taxonomy of the producing streptomycete and isolation of the active principle. *The Journal of Antibiotics*, 28(10), pp.721-726.

Williams, A., Werner-Fraczek, J., Chang, I. and Bailey-Serres, J., 2003. Regulated Phosphorylation of 40S Ribosomal Protein S6 in Root Tips of Maize. *Plant Physiology*, 132(4), pp.2086-2097.

Winter, D., Vinegar, B., Nahal, H., Ammar, R., Wilson, G. and Provart, N., 2007. An "Electronic Fluorescent Pictograph" Browser for Exploring and Analyzing Large-Scale Biological Data Sets. *PLoS ONE*, 2(8), p.e718.

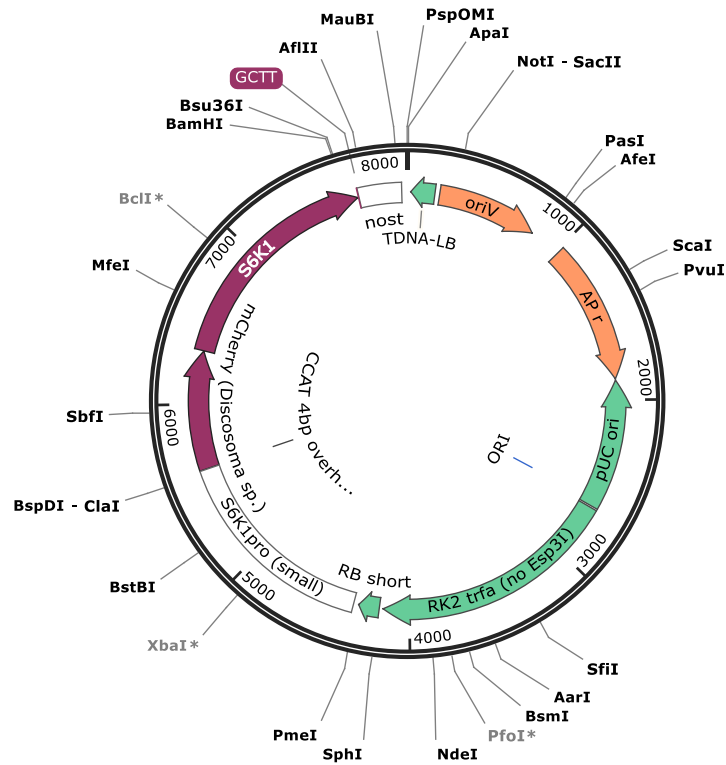
Yaguchi, M., Ikeya, S. and Kozaki, A., 2019. The activation mechanism of plant S6 kinase (S6K), a substrate of TOR kinase, is different from that of mammalian S6K. *FEBS Letters*, 594(4), pp.776-787.

Zhang, S. H., Broome, M. A., Lawton, M. A., Hunter, T., and Lamb, C. J., 1994a. *atpk1*, a novel ribosomal protein kinase gene from *Arabidopsis*. II. Functional and biochemical analysis of the encoded protein. *J. Biol. Chem.* 269 (26), 17593–17599. doi:10.1016/s0021-9258(17)32482-1.

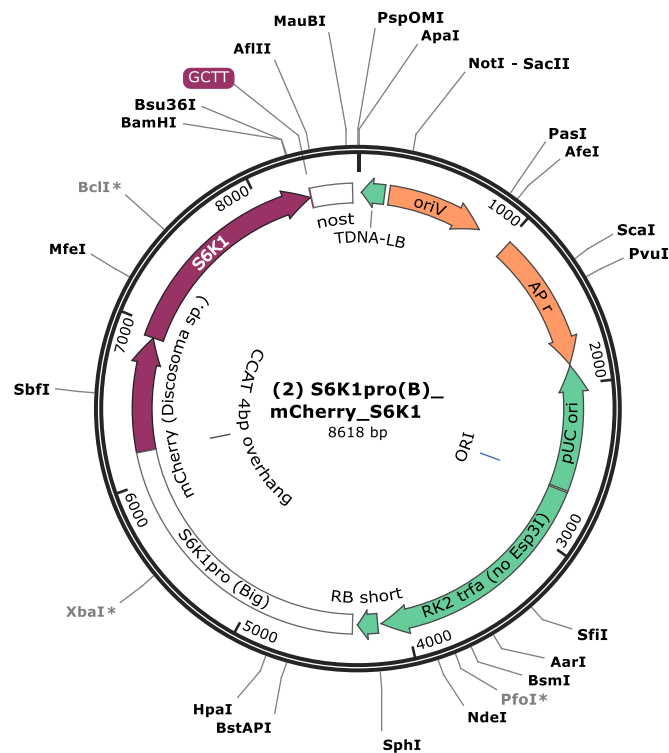
Zhang, S. H., Lawton, M. A., Hunter, T., and Lamb, C. J., 1994b. *atpk1*, a novel ribosomal protein kinase gene from *Arabidopsis*. I. Isolation, characterization, and expression. *J. Biol. Chem.* 269 (26), 17586–17592. doi:10.1016/s0021-9258(17)32481-x.

Zhang, Z., Zhu, J., Roh, J., Marchive, C., Kim, S., Meyer, C., Sun, Y., Wang, W. and Wang, Z., 2016. TOR Signaling Promotes Accumulation of BZR1 to Balance Growth with Carbon Availability in *Arabidopsis*. *Current Biology*, 26(14), pp.1854-1860.

Appendices



(1) S6K1pro(S)_mCherry_S6K1
8027 bp



(2) S6K1pro(B)_mCherry_S6K1
8618 bp

Appendix A and B. Plasmid map of mCherry tagged S6K1 constructs with varying promoters.


```

AtS6K1      VSSQRVPVFNKIQQQYLSISPSNSVLKDDVELEFSDVFGPLPEANDIAYDEPAVVYSRSHSLVGP CSLDSSHSLKLTKLT
F_T7       VSSQRVPVFNKIQQQYLSISPSNSVLKDDVELEFSDVFGPLPEANDIAYDEPAVVYSRSHSLVGP CSLDSSHSLKLTKLT
F_T7term   -----

AtS6K1      LLETEDSIDLVECLEGESLKENDDFSGNDDSDNEKALEGDLVKVSGVVGIDDFEVMKVVGKGFAGKVIQVRKKETSEIYA
F_T7       LLETEDSIDLVECLEGESLKENDDFSGNDDSDNEKALEGDLVKVSGVVGIDDFEVMKVVGKGFAGKVIQVRKKETSEIYA
F_T7term   -----

AtS6K1      *****
F_T7       MKVMRKDHIMEKNHAEYMKAERDILTKIDHPFIVQLKYSFQTKYRLYLVLDFINGGHLFFQLYHQGLFREDLARVYTAEI
F_T7term   MKVMRKDHIMEKNHAEYMKAERDILTKIDHPFIVQLKYSFQTKYRLYLVLDFINGGHLFFQLYHQGLFREDLARVYTAEI
-----MKAERDILTKIDHPFIVQLKYSFQTKYRLYLVLDFINGGHLFFQLYHQGLFREDLARVYTAEI

AtS6K1      *****
F_T7       VSAVSHLHEKGIIMHRDLKPENILMDTDGHVMLTDFGLAKEFEENTRSNSMCGTTEYMAPEIVRGKGDKAADWWSVGILL
F_T7term   VSAVSHLHEKGIIMHRDLKPENILMDTDGHVMLTDFGLAKEFEENTRSNSMCGTTEYMAPEIVRGKGDKAADWWSVGILL
-----VSAVSHLHEKGIIMHRDLKPENILMDTDGHVMLTDFGLAKEFEENTRSNSMCGTTEYMAPEIVRGKGDKAADWWSVGILL

AtS6K1      YEMLTGKPPFLGSKGKIQQKIVKDKIKLPQFLSNEAHAILKGLLQKEPERRLGSGLSGAEEIKQHKWFKGINWKKLEARE
F_T7       YEMLTGKPPFLGSKGKIQQKIVKDKIKLPQFLSNEAHAILKGLLQKEPERRLGSGLSGAEEIKQHKWFKGINWKKLEARE
F_T7term   -----

AtS6K1      VMPSFKPEVSGRQCIANFDKCWTDMSVLDSPASSPSSDPKANPFTNFTYVVRPPPSFLHQSTTLL-----
F_T7       VMPSFKPEVSGRQCIANFDKCWTDMSVLDSPASSPSSDPKANPFTNFTYVVRPPPSFLHQSTTLL-----
F_T7term   VMPSFKPEVSGRQCIANFDKCWTDMSVLDSPASSPSSDPKANPFTNFTYVVRPPPSFLHQSTTLL EHHHHHH

```

Appendix G Multiple sequence alignments of AtS6k1 F construct in Pet-21a (+) vector.

The generated DNA plasmids were amplified and purified prior to sequencing by Eurofins. Received sequences were aligned and analysed for correct construction. AtS6K1 sequence obtained from UniProt is depicted as AtS6K1_Seq. AtS6K1_T7 and AtS6K1_T7TERM are stored primers used by Eurofins to sequence the beginning and the end of the gene respectively.

```

AtS6K1      NEKALEGDLVKVSGVVGIDDFEVMKVVGKGAFGKVYQVRKKEITSEIYAMKVMRKHIMEKNHAEYMKAEIRDILTKIDHPPF
KL_T7      NEKALEGDLVKVSGVVGIDDFEVMKVVGKGAFGKVYQVRKKEITSEIYAMKVMRKHIMEKNHAEYMKAEIRDILTKIDHPPF
KL_T7term  -----MKVMRKHIMEKNHAEYMKAEIRDILTKIDHPPF

AtS6K1      IVQLKYSFQTKYRLYLVLDFINGGHLFFQLYHQGLFREDLARVYTAEIVSAVSHLHEKIGIMHRDLKPENILMDTDGHVML
KL_T7      IVQLKYSFQTKYRLYLVLDFINGGHLFFQLYHQGLFREDLARVYTAEIVSAVSHLHEKIGIMHRDLKPENILMDTDGHVML
KL_T7term  IVQLKYSFQTKYRLYLVLDFINGGHLFFQLYHQGLFREDLARVYTAEIVSAVSHLHEKIGIMHRDLKPENILMDTDGHVML

AtS6K1      TDFGLAKEFEENTRSNSMCGTEYMAPEIVRGKGHDKAADWWSVGILLYEMLTGKPPFLGSKGKIQQKIVKDKIKLPQFL
KL_T7      TDFGLAKEFEENTRSNSMCGTEYMAPEIVRGKGHDKAADWWSVGILLYEML-----
KL_T7term  TDFGLAKEFEENTRSNSMCGTEYMAPEIVRGKGHDKAADWWSVGILLYEMLTGKPPFLGSKGKIQQKIVKDKIKLPQFL

AtS6K1      SNEAHAILKGLLOKEPERRLGSLGSAEEIKQHKWFKGINWKKLEAREVMPSPFKPEVSGROCIANFDKCWTDMSVLDSPA
KL_T7      SNEAHAILKGLLOKEPERRLGSLGSAEEIKQHKWFKGINWKKLEAREVMPSPFKPEVSGROCIANFDKCWTDMSVLDSPA
KL_T7term  SNEAHAILKGLLOKEPERRLGSLGSAEEIKQHKWFKGINWKKLEAREVMPSPFKPEVSGROCIANFDKCWTDMSVLDSPA

AtS6K1      SSPSSDPKANPFTNFTYVRPPPSFLHQSTTTL-----
KL_T7      -----
KL_T7term  SSPSSDPKANPFTNFTYVRPPPSFLHQSTTTLLEHHHHHH

```

Appendix H Multiple sequence alignments of AtS6k1 KL construct in Pet-21a (+) vector.

The generated DNA plasmids were amplified and purified prior to sequencing by Eurofins. Received sequences were aligned and analysed for correct construction. AtS6K1 sequence obtained from UniProt is depicted as AtS6K1_Seq. AtS6K1_T7 and AtS6K1_T7TERM are stored primers used by Eurofins to sequence the beginning and the end of the gene respectively.

```

*****
AtS6K1      NEKALEGLVKVSGVVGIDDFEVMKVVGKGFAGKVIQVRKKETSEIYAMKVMRKHIMEKNHAEYMKAEIRDILTKIDHPP
Ka_T7      NEKALEGLVKVSGVVGIDDFEVMKVVGKGFAGKVIQVRKKETSEIYAMKVMRKHIMEKNHAEYMKAEIRDILTKIDHPP
Ka_T7term  NEKALEGLVKVSGVVGIDDFEVMKVVGKGFAGKVIQVRKKETSEIYAMKVMRKHIMEKNHAEYMKAEIRDILTKIDHPP

*****
AtS6K1      IVQLKYSFQTKYRLYLVLDFINGGHLFFQLYHQGLFREDLARVYTAEIVSAVSHLHEKIGIMHRDLKPENILMDTDGHVML
Ka_T7      IVQLKYSFQTKYRLYLVLDFINGGHLFFQLYHQGLFREDLARVYTAEIVSAVSHLHEKIGIMHRDLKPENILMDTDGHVML
Ka_T7term  IVQLKYSFQTKYRLYLVLDFINGGHLFFQLYHQGLFREDLARVYTAEIVSAVSHLHEKIGIMHRDLKPENILMDTDGHVML

*****
AtS6K1      TDFGLAKEFEENTRSNSMCGTEYMAPEIVRGKGHDKAADWWSVGILLYEMLTGKPPFLGSKGKIQQKIVKDKIKLPQFL
Ka_T7      TDFGLAKEFEENTRSNSMCGTEYMAPEIVRGKGHDKAADWWSVGILLYEMLTGKPPFLGSKGKIQQKIVKDKIKLPQFL
Ka_T7term  TDFGLAKEFEENTRSNSMCGTEYMAPEIVRGKGHDKAADWWSVGILLYEMLTGKPPFLGSKGKIQQKIVKDKIKLPQFL

*****
AtS6K1      SNEAHAILKGLLOKEPERRLGSLGAEIIRQHKWFKGINWKKLEAREVMPSPF
Ka_T7      SNEAHAILKGLLOKEPERRLGSLGAEIIRQHKWFKGINWKKLEAREVMPSPF
Ka_T7term  SNEAHAILKGLLOKEPERRLGSLGAEIIRQHKWFKGINWKKLEAREVMPSPF

```

Appendix I Multiple sequence alignments of AtS6k1 K construct in Pet-21a (+) vector.

The generated DNA plasmids were amplified and purified prior to sequencing by Eurofins. Received sequences were aligned and analysed for correct construction. AtS6K1 sequence obtained from UniProt is depicted as AtS6K1_Seq. AtS6K1_T7 and AtS6K1_T7TERM are stored primers used by Eurofins to sequence the beginning and the end of the gene respectively.